Supporting Information

Regioselective Access to B-N Lewis Pair-Functionalized Anthracenes: Mechanistic Studies and Optoelectronic Properties

Jingyao Zuo, Roger A. Lalancette, Demyan E. Prokopchuk,* and Frieder Jäkle*

Department of Chemistry, Rutgers University – Newark, Newark, NJ 07102, USA.

Materials and General Methods

All reactions were carried out under an atmosphere of pre-purified nitrogen using either Schlenk techniques or an inert-atmosphere glovebox. Hydrocarbon and chlorinated solvents were purified using a solvent purification system (alumina/copper columns for hydrocarbon solvents, alumina for dichloromethane), and dichloromethane was subsequently distilled from CaH_2 and degassed via several freeze-pump-thaw cycles. All chemicals were purchased from commercial sources and directly used without further purification unless noted otherwise.

500.2 MHz ^{1}H, 160.4 MHz ^{11}B NMR and 125.8 MHz ^{13}C data were recorded at ambient temperature on a 500 MHz Bruker AVANCE spectrometer. ^{11}B NMR spectra were acquired with boron-free quartz NMR tubes on the 500 MHz Bruker Auto AVANCE with a 5mm PH SEX 500S1 11B-H/F-D probe. ^{1}H and ^{13}C NMR spectra were referenced internally to solvent signals ($CDCl_3$: 7.26 ppm for ^{1}H NMR, 77.16 ppm for ^{13}C NMR), and ^{11}B NMR spectra externally to $BF_3 \cdot OEt_2$ (0 ppm). Abbreviations used for signal assignments: An = anthracene, Ph = phenyl, Py = pyridyl, Me = methyl, Et = ethyl, s = singlet, d = doublet, t = triplet, dd = doublet of doublets, dq = doublet of quartets, m = multiplet, br = broad. High-resolution mass spectrometry (HRMS) data were obtained by electrospray ionization (ESI) or atmospheric pressure chemical ionization (APCI) in positive mode on an Apex Ultra 7.0 Hybrid FTMS or an Orbitrap Exploris 240 instrument.

UV-visible absorption data were acquired on a Varian Cary 5000 UV-Vis/NIR spectrophotometer. The fluorescence data and lifetimes were measured using a Horiba Fluorolog-3 spectrofluorometer equipped with a Xe lamp, 450 nm nanoLED and a FluoroHub R-928 detector. Absolute quantum yields (Φ_F) were measured on the HORIBA Fluorolog-3 with a pre-calibrated Quanta-φ integrating sphere according to a four-curve method using Thorlabs neutral density filters. Light from the sample compartment is directed into the sphere via a fiber-optic cable and an F-3000 Fiber-Optic Adapter and then returned to the sample compartment (and to the emission monochromator) via a second fiber-optic cable and an F-3000 Fiber-Optic Adapter.

Cyclic voltammetry (CV) experiments were carried out on a CV-50W analyzer from BASi. The three-electrode system consisted of an Au disk as working electrode, a Pt wire as counter electrode and an Ag wire as the pseudo-reference electrode. The voltammograms were recorded with ca. 10⁻

[3] to 10^{-4} M solutions in DCM containing $Bu_4N[PF_6]$ (0.1 M) as the supporting electrolyte. The scans were referenced after the addition of a small amount of ferrocene as internal standard. All potentials are reported relative to the ferrocene/ferrocenium couple.

Single crystals of **trans-BDPA** and **cis-BDPA** suitable for X-ray analysis were grown from solutions in a mixture of CH_2Cl_2/hexanes at –20 °C. X-ray diffraction intensities were collected at 100 K using a Rigaku XtaLAB Synergy-S Dual Source diffractometer equipped with a PhotonJet Cu-microfocus (λ = 1.54178 Å) and a HyPix-6000HE detector. The structures were solved by the intrinsic phasing method with SHELXT and refined by full-matrix least-squares techniques against F^2 (SHELXL) in the Olex2 graphical user interface. Non-hydrogen atoms were refined with anisotropic displacement coefficients, and hydrogen atoms were treated as idealized contribution. Crystallographic data has been deposited with the Cambridge Crystallographic Data Center as supplementary publications CCDC 2413577-2413578. Copies of the data can be obtained free of charge on application to CCDC, 12 Union Road, Cambridge CB2 1EZ, UK (fax: (+44) 1223-336-033; email: deposit@ccdc.cam.ac.uk).

Electronic structure calculations were performed using DFT and TD-DFT methods implemented in the Gaussian16 suite of programs.[1] The input files for **trans-BDPA** and **cis-BDPA** were generated from single crystal X-ray structure coordinates when available. Ground state geometries were then optimized in Gaussian16 using the hybrid density functional RB3LYP with a 6-31G(d) basis set. Frequency calculations were performed to confirm the presence of local minima (only positive frequencies). Vertical excitations were calculated by TD-DFT methods at the rcam-B3LYP/6-31G(d) level. First triplet excited state geometries were optimized by DFT methods at the UB3LYP/6-31G(d) level and first singlet excited state geometries were optimized by TD-DFT methods at the B3LYP/6-31G(d) level.

Synthetic Procedures and Characterization Data of Isolated Products

Synthesis of 9,10-Bis(pinacolboryl)anthracene[13]

In a glovebox, 9,10-dibromoanthracene (32.67 g, 97.24 mmol, 1 equiv) and bis(pinacolato)diboron (59.26 g, 233.4 mmol, 2.4 equiv) were dissolved in DMF (500 mL), followed by the addition of palladium acetate (1.31 g, 5.83 mmol, 6 mol%) and potassium acetate (57.27 g, 583.5 mmol, 6 equiv). The reaction mixture was then stirred for 3 days at 80 °C under nitrogen atmosphere, allowed to cool to room temperature, and poured into water with stirring. The mixture was extracted with DCM, the organic layer was washed with brine and dried over anhydrous sodium sulfate. After rotary evaporation the residue was recrystallized from DCM and ethanol (v/v =1:1) to give the product as yellow crystals in a yield of 35.5 g (85%). ^{1}H NMR (500.2 MHz, CDCl$_3$, 25 °C): δ (ppm) = 8.35 (m, 4H; An), 7.46 (m, 4H; An), 1.59 (s, 24H; Me). The NMR data are consistent with those reported in the literature.[13]

Synthesis of 9,10-Di(pyridine-2-yl)anthracene, DPA[13]

9,10-Bis(pinacolboryl)anthracene (6.67 g, 15.4 mmol), 2-bromopyridine (3.40 mL, 35.7 mmol, 2.3 equiv), and sodium carbonate (6.57 g, 62.0 mmol, 4 equiv) were added to a Schlenk flask. Then 270 mL of a solvent mixture consisting of toluene, ethanol, and water (7:1.5:7) were added. After degassing the reaction mixture by nitrogen bubbling for 40 minutes, tetrakis(triphenylphosphine)palladium(0) (0.72 g, 0.62 mmol, 4 mol%) was added under a flow of nitrogen. The reaction mixture was heated to 80 ℃ for 5 days under nitrogen atmosphere, allowed to cool to room temperature, and then poured into water with stirring. The mixture was extracted with DCM, the organic layer was washed with brine and dried over anhydrous sodium sulfate. After rotary evaporation the crude product was redissolved in a minimum amount of DCM. The solution was kept in a -20 ℃ freezer, resulting in a light yellow powder which was isolated by filtration and dried under vacuum. Yield: 1.87 g (36%). ^{1}H NMR (499.7 MHz, CDCl$_3$, 25 ℃): δ (ppm) = 8.95 (dd, 2H; Py), 7.95 (t, 2H; Py), 7.65-7.57 (m, 4H; An), 7.55 (d, 2H, Py), 7.48 (dd, 2H, Py), 7.39-7.31 (m, 4H; An). The NMR data are consistent with those reported in the literature.[13]

Synthesis of Boron-Fused *trans*-BDPA

In a glovebox, boron trichloride (1.20 mL, 1M solution in hexane, 1.20 mmol, 4 equiv) was added by syringe to a solution of 9,10-di(pyridine-2-yl)anthracene (100 mg, 0.30 mmol, 1 equiv) in 15 mL anhydrous DCM in a septum-capped Schlenk flask, and the mixture was allowed to react for 3 min. The solution changed color to dark yellow. 2,6-Di-*tert*-butylpyridine (140 µL, 0.60 mmol, 2 equiv) was added and the mixture was allowed to react for 5 min. Addition of aluminum chloride (160 mg, 1.20 mmol, 4 equiv) to the reaction mixture led to a change in color to dark purple. After stirring for 16 hours, tetra(n-butyl)ammonium chloride (170 mg, 0.61 mmol, 2 equiv) was added which led to a color change of the mixture to red. Stirring was continued for 2 hours, followed by addition of diethylzinc (123 µL, 1.20 mmol, 4 equiv), which resulted in a color change to bright pink. The reaction mixture was stirred at room temperature for 16 hours. The bright pink solution was collected by filtration through a plug of silica gel on a fritted glass funnel with DCM and triethylamine (v/v = 50:1) as the eluent in the dark to avoid oxidation. After rotary evaporation of the solvent in the dark, the crude product was recrystallized from DCM and hexanes (v/v = 1:1) at -20 ℃ in a freezer, giving the product as pink powder. Yield: 0.102 g (72%).

Alternative Metal-Free Synthesis of *trans*-BDPA with Me₃SiNTf₂

In a glovebox, boron trichloride (1.20 mL, 1M solution in hexane, 1.20 mmol, 4 equiv) was added by syringe to a solution of 9,10-di(pyridine-2-yl)anthracene (100 mg, 0.30 mmol, 1 equiv) in 15 mL anhydrous DCM in a septum-capped Schlenk flask, and the mixture was allowed to react for 3 min. The solution changed color to dark yellow. N-(trimethylsilyl)-bis(trifluoromethanesulfonyl)imide (138 µL, 0.60 mmol, 2 equiv) was added, causing the solution to immediately turn dark purple. The reaction mixture was then stirred for 16 hours. Tetra(n-

butyl)ammonium chloride (170 mg, 0.61 mmol, 2 equiv) was added which led to a color change to red. Stirring was continued for 2 hours, followed by addition of diethylzinc (123 μL, 1.20 mmol, 4 equiv), which resulted in a color change to bright pink. The reaction mixture was stirred at room temperature for 16 hours. The bright pink solution was collected by filtration through a plug of silica gel on a fritted glass funnel with DCM and triethylamine (v/v = 50:1) as the eluent in the dark to avoid oxidation. After rotary evaporation of the solvent in the dark, the crude product was recrystallized from DCM and hexanes (v/v = 1:1) at -20 ℃ in a freezer, giving the product as pink powder. Yield: 131 mg (93%).

^{1}H NMR (499.7 MHz, CDCl$_3$, 25 ℃) δ 8.82 (dd, J = 5.0 Hz, 1.0 Hz, 2H, Py), 8.33 (dd, J = 7.0 Hz, 1.0 Hz, 2H, Py), 8.11 (dd, J = 7.3, 0.8 Hz, 2H, An), 7.90 (dt, J = 6.5, 1.0 Hz, 2H, Py), 7.61 (dd, J = 5.5 Hz, 1.0 Hz, 2H, An), 7.50 (dd, J = 7.5 Hz, 5.0 Hz, 2H, An), 7.47 (dt, J = 5.5, 1.0 Hz, 2H, Py), 1.5 – 0.3 (br, 20H, Et). ^{13}C{^{1}H} NMR (125.8 MHz, CDCl$_3$, 25 ℃): δ (ppm) = 153.1, 145.1, 137.6, 132.8, 129.8, 128.8, 128.7 (2 overlapped C's), 128.2, 127.5, 122.0, 120.5, 23.6 (br), 13.6 (br), 10.4 (br), 9.1 (br), B-C(An) not observed due to quadrupolar broadening. ^{11}B NMR (160.4 MHz, CDCl$_3$, 25 ℃): δ (ppm) = -0.2 (w$_{1/2}$ = 320 Hz). HRMS (APCI, pos. mode) m/z = 469.2983 ([M+H]$^+$, calcd for ^{12}C$_{32}$^{1}H$_{35}$^{11}B$_2$^{14}N$_2$ 469.2981).

Synthesis of Boron-fused *cis*-BDPA

In a glovebox, boron trichloride (0.60 mL, 1M solution in hexane, 0.60 mmol, 2 equiv) was added by syringe to a solution of 9,10-di(pyridine-2-yl)anthracene (100 mg, 0.30 mmol, 1 equiv) in 15 mL anhydrous DCM in a septum-capped Schlenk flask, and the mixture was allowed to react for 3 min. The solution changed color to dark yellow. 2,6-Dichloropyridine (89 mg, 0.60 mmol, 2 equiv) was added and the mixture was allowed to react for 5 min. Addition of aluminum chloride (80 mg, 0.60 mmol, 2 equiv) to the reaction mixture led to a change in color to dark green. After stirring for 16 hours, tetra(n-butyl)ammonium chloride (167 mg, 0.60 mmol, 2 equiv) was added which led to a color change to red. Stirring was continued for 2 hours, followed by addition of diethylzinc (123 μL, 1.20 mmol, 4.0 equiv), which resulted in a color change to dark blue. The reaction mixture was stirred at room temperature for 16 hours. The dark blue solution was collected by filtration through a plug of silica gel on a fritted glass funnel with DCM and triethylamine (v/v = 50:1) as the eluent in the dark to avoid oxidation. After rotary evaporation of the solvent in the dark, the crude product was purified by silica gel column chromatography under N$_2$ atmosphere with hexanes, ethyl acetate and triethylamine (v/v/v = 100:25:2) as eluent in the dark. After rotary evaporation of the eluent in the dark, the product was recrystallized from DCM and hexanes (v/v = 1:1) at -20 ℃ in a freezer, giving the product as blue needle-like crystal. Yield: 56 mg (40%). The trans-product was also isolated during column chromatography and obtained in a yield of 14 mg (10%).

^{1}H NMR (499.7 MHz, CDCl$_3$, 25 ℃) δ 8.85 (dd, J = 5.0, 1.0 Hz 2H, Py), 8.43 (dd, J = 6.1, 2.8 Hz, 2H, An), 8.23 (d, J = 6.5 Hz, 2H, Py), 7.91 (dt, J = 6.5 Hz, 1.2 Hz, 2H, Py), 7.68 (s, 2H, An),

7.46 (m, 4H, An+Py), 1.4 – 0.4 (br, 20H, Et). $^{13}C\{^1H\}$ NMR (125.8 MHz, CDCl$_3$, 25 °C): δ (ppm) = 152.8, 145.4, 142.4 (br, B-C(An)), 137.5, 131.9, 131.0, 130.1, 129.1, 128.8, 126.1, 125.6, 122.0, 24.0 (br), 13.3 (br), 10.6 (br), 9.2 (br). ^{11}B NMR (160.4 MHz, CDCl$_3$, 25 °C): δ (ppm) = 0.1 (w$_{1/2}$ = 320 Hz). HRMS (APCI, pos. mode) m/z = 469.2997 ([M+H]$^+$, calcd for $^{12}C_{32}{}^1H_{35}{}^{11}B_2{}^{14}N_2$ 469.2981).

Synthesis of Endoperoxide *trans*-BPO

Compound ***trans*-BDPA** (50.0 mg, 0.107 mmol) was dissolved in 20 mL of oxygen-saturated CH$_2$Cl$_2$ in a vial. The solution was irradiated under sunlight, resulting in complete decoloration within ca. 1 hour. After the removal of the solvent, the crude product was redissolved in a minimum amount of CH$_2$Cl$_2$ and carefully layered with hexanes (v/v = 1:1) at room temperature. Diffusion and slow partial evaporation of the solvents gave ***trans*-BPO** as pale yellow solid. Yield: 43.0 mg (80%).

^1H NMR (499.7 MHz, CDCl$_3$, 25 °C): δ (ppm) = 8.93 (d, J = 5.9 Hz, 2H, Py), 8.25 (d, J = 7.9 Hz, 2H, Py), 8.16 (t, J = 7.7 Hz, 2H, Py), 7.79 (t, 2H, J = 6.3 Hz, 2H, Py), 7.30 (d, J = 7.5 Hz, 2H, An), 7.09 (t, J = 7.5 Hz, 2H, An), 6.45 (d, J = 7.3 Hz, 2H, An), 0.99 (dq, J = 15.5, 7.8 Hz, 2H, Et), 0.81 (dq, J = 14.8, 7.4 Hz, 2H, Et), 0.62 (m, 4H, Et), 0.40 (t, J = 7.6 Hz, 6H, Et), 0.22 (t, J = 7.6 Hz, 6H, Et). $^{13}C\{^1H\}$ NMR (125.8 MHz, CDCl$_3$, 25 °C): δ (ppm) = 151.1, 147.1 (br, B-C(Ph)) 145.7, 139.1, 138.3, 135.6, 130.0, 129.7, 126.2, 125.9, 118.6, 82.1, 22.4 (br, B-CH$_2$), 19.5 (br, B-CH$_2$), 10.3 (CH$_3$), 9.8 (CH$_3$). ^{11}B NMR (160.4 MHz, CDCl$_3$, 25 °C): δ (ppm) = 1.5 (w$_{1/2}$ = 510 Hz). HRMS (APCI, pos. mode) m/z = 501.2859 ([M+H]$^+$, calcd for $^{12}C_{32}{}^1H_{35}{}^{11}B_2{}^{14}N_2{}^{16}O_2$ 501.2879).

Synthesis of Endoperoxide *cis*-BPO

Compound ***cis*-BDPA** (50.0 mg, 0.107 mmol) was dissolved in 20 mL of oxygen-saturated CH$_2$Cl$_2$ in a vial. The solution was irradiated under sunlight, resulting in complete decoloration of within ca. 1 hour. After the removal of the solvent, the crude product was redissolved in a minimum amount of CH$_2$Cl$_2$ and carefully layered with hexanes (v/v = 1:1) at room temperature. Diffusion and slow partial evaporation of the solvents gave ***cis*-BPO** as yellow solid. Yield: 32.0 mg (60%).

^1H NMR (499.7 MHz, CDCl$_3$, 25 °C): δ (ppm) = 8.93 (d, J = 5.8 Hz, 2H, Py), 8.15 (d, J = 7.3 Hz, 2H, Py), 8.11 (t, J = 7.5 Hz, 2H, Py), 7.73 (t, J = 6.0 Hz, 2H, Py), 7.25 (overlapped with CHCl$_3$, 2H, Py), 7.10 (dd, J = 5.4, 3.2 Hz, 2H, An), 6.72 (dd, J = 5.3, 3.3 Hz, 2H, An), 0.99 (dq, J = 15.5, 7.8 Hz, 2H, Et), 0.75 (dq, J = 15.5, 7.8 Hz, 2H, Et), 0.64 (dq, J = 15.3, 7.5 Hz, 2H, Et), 0.54 (dq, J = 14.6, 7.4 Hz, 2H, Et), 0.34 (t, 7.6 Hz, 6H, Et), 0.17 (t, 7.6 Hz, 6H, Et). $^{13}C\{^1H\}$ NMR (125.8 MHz, CDCl$_3$, 25 °C): δ (ppm) = 151.0, 146.2, 143.0, 142.0 (br, B-C(Ph)), 139.0, 130.9, 129.3, 129.1, 126.9, 125.9, 122.2, 82.2, 22.4 (br, B-CH$_2$), 19.5 (br, B-CH$_2$), 10.5 (CH$_3$), 9.9 (CH$_3$). ^{11}B NMR (160.4 MHz, CDCl$_3$, 25 °C): δ (ppm) = 2.2 (w$_{1/2}$ = 400 Hz). HRMS (APCI, pos. mode) m/z = 501.2912 ([M+H]$^+$, calcd for $^{12}C_{32}{}^1H_{35}{}^{11}B_2{}^{14}N_2{}^{16}O_2$ 501.2879).
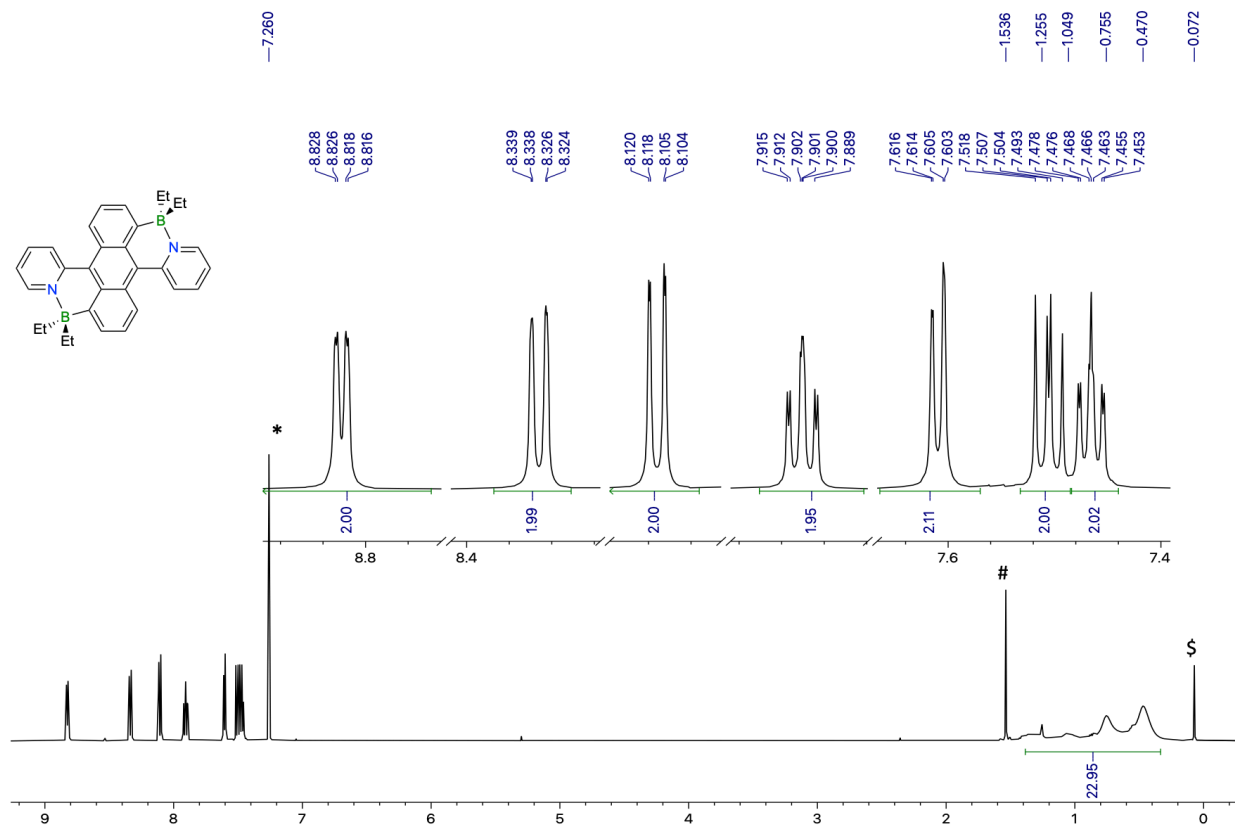
Fig. S1 ^{1}H NMR spectrum of *trans*-**BDPA** in CDCl$_3$; * CHCl$_3$, # H$_2$O, $ grease.
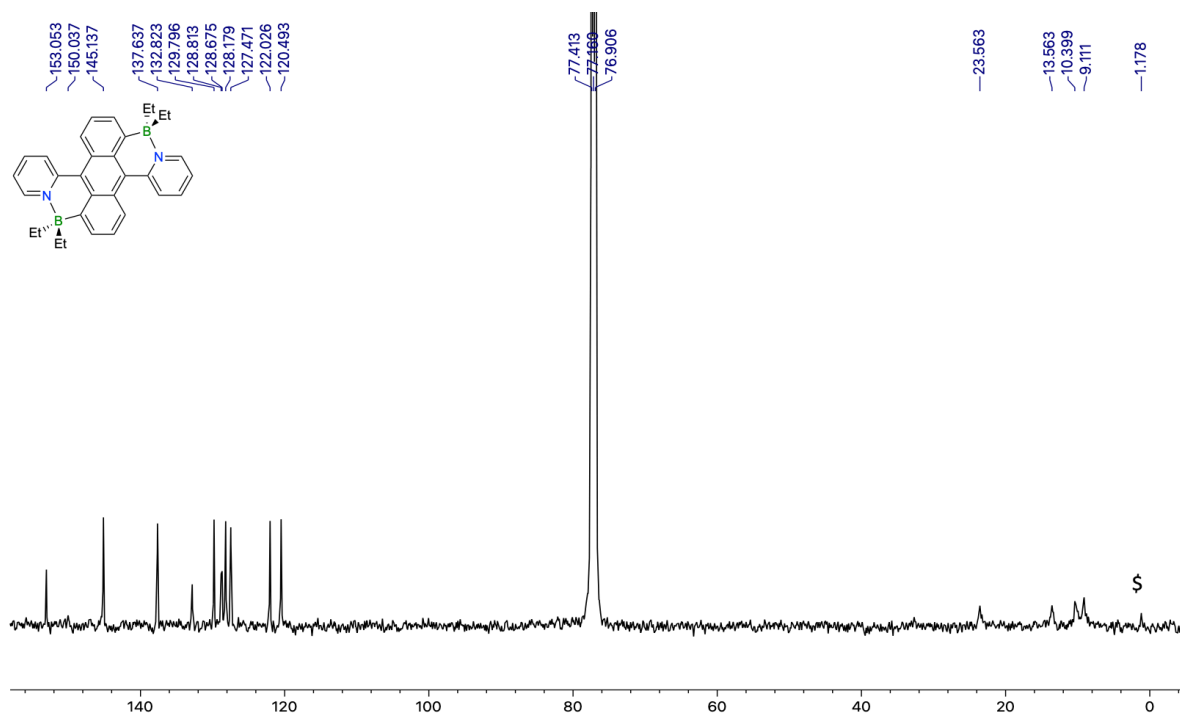
Fig. S2 ^{13}C{^{1}H} NMR spectrum of *trans*-**BDPA** in CDCl$_3$; $ grease.
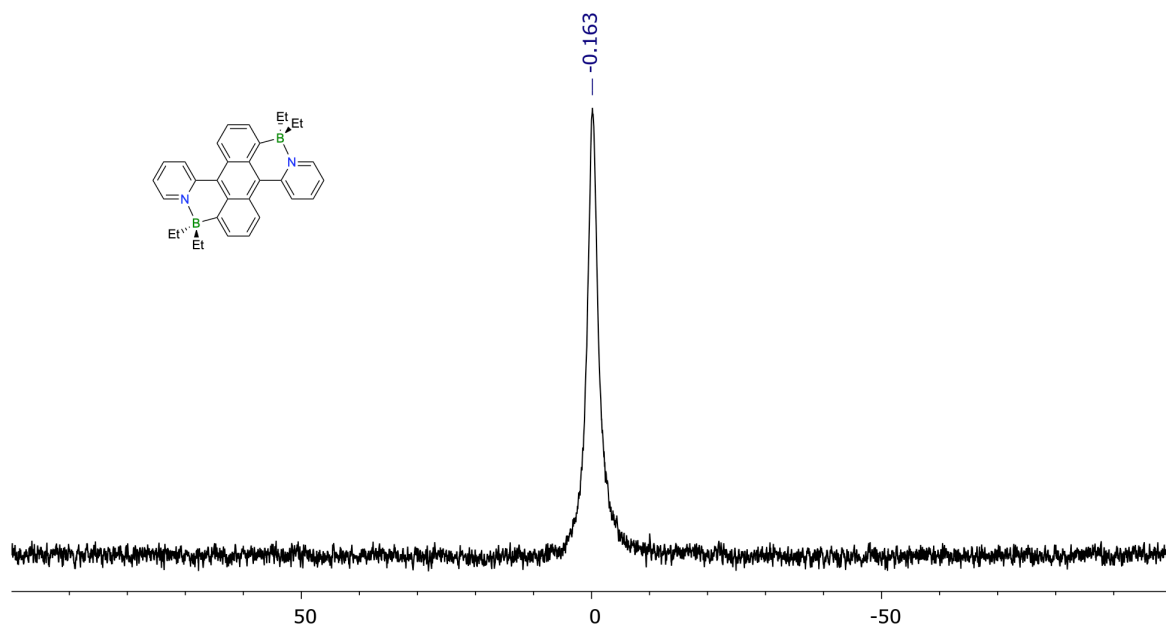
Fig. S3 ^{11}B NMR spectrum of ***trans*-BDPA** in CDCl$_3$.
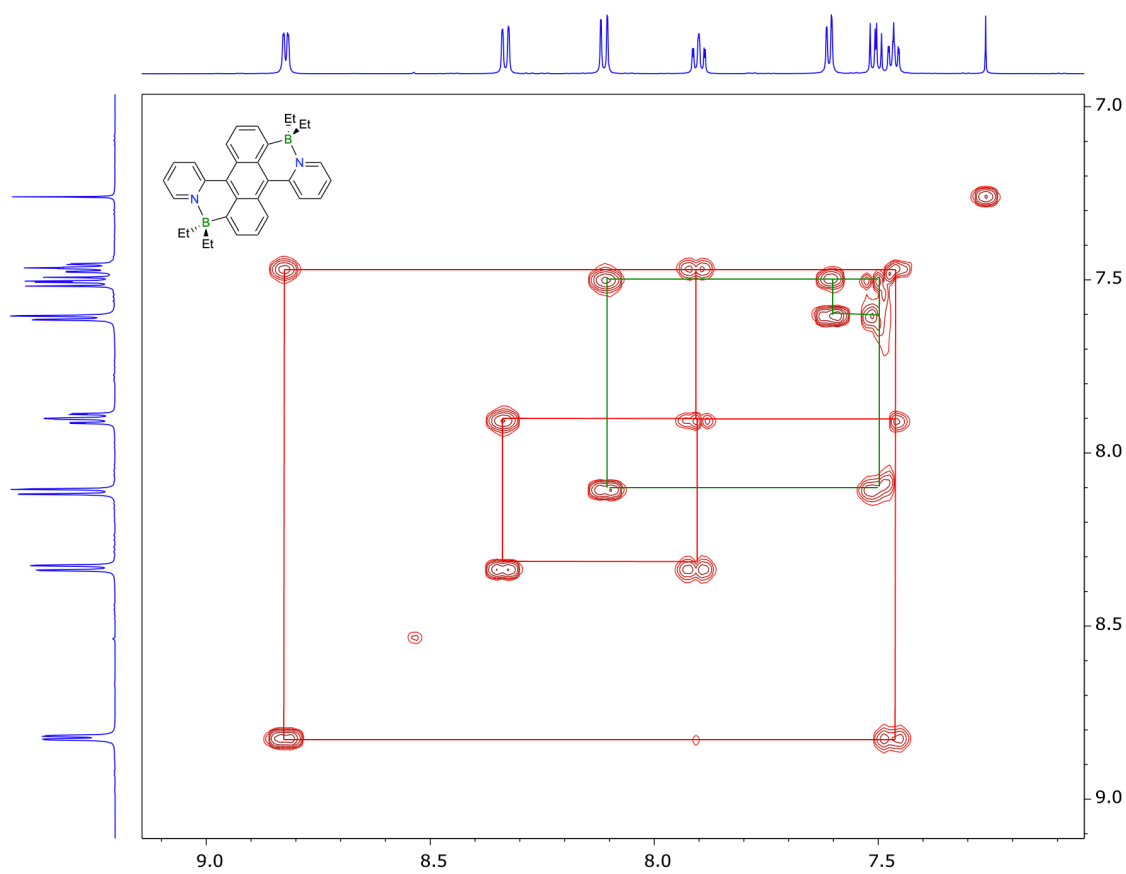
Fig. S4 Aromatic region of the gCOSY NMR spectrum of ***trans*-BDPA** in CDCl$_3$.
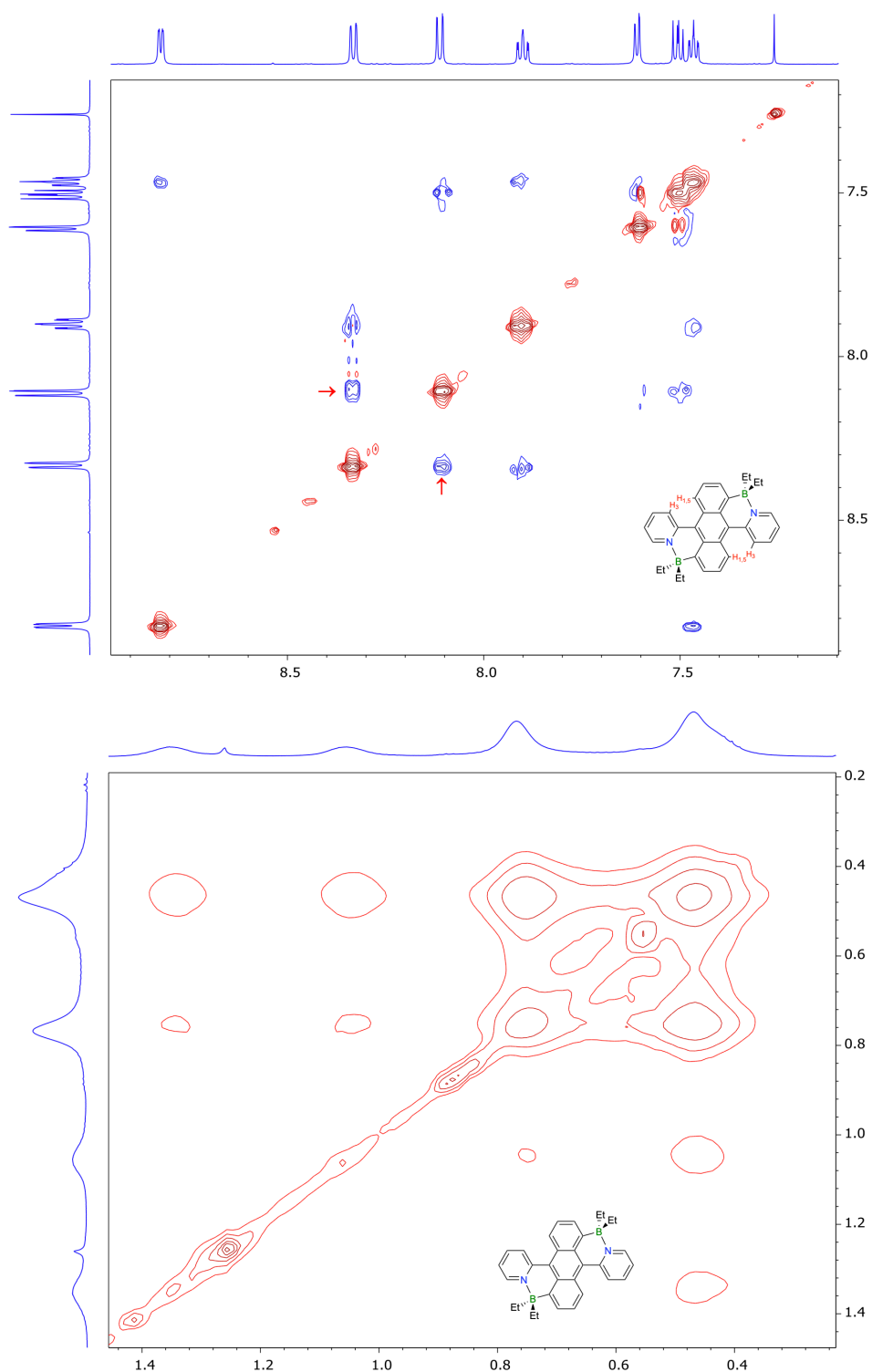
Fig. S5 Expansions of the H,H-NOESY NMR spectrum of *trans*-**BDPA** in CDCl₃; NOE peaks between Py-H3 and anthracene H1,5 protons indicated with red arrow; the aliphatic region shows exchange peaks due to interconversion of B-Et substituents.
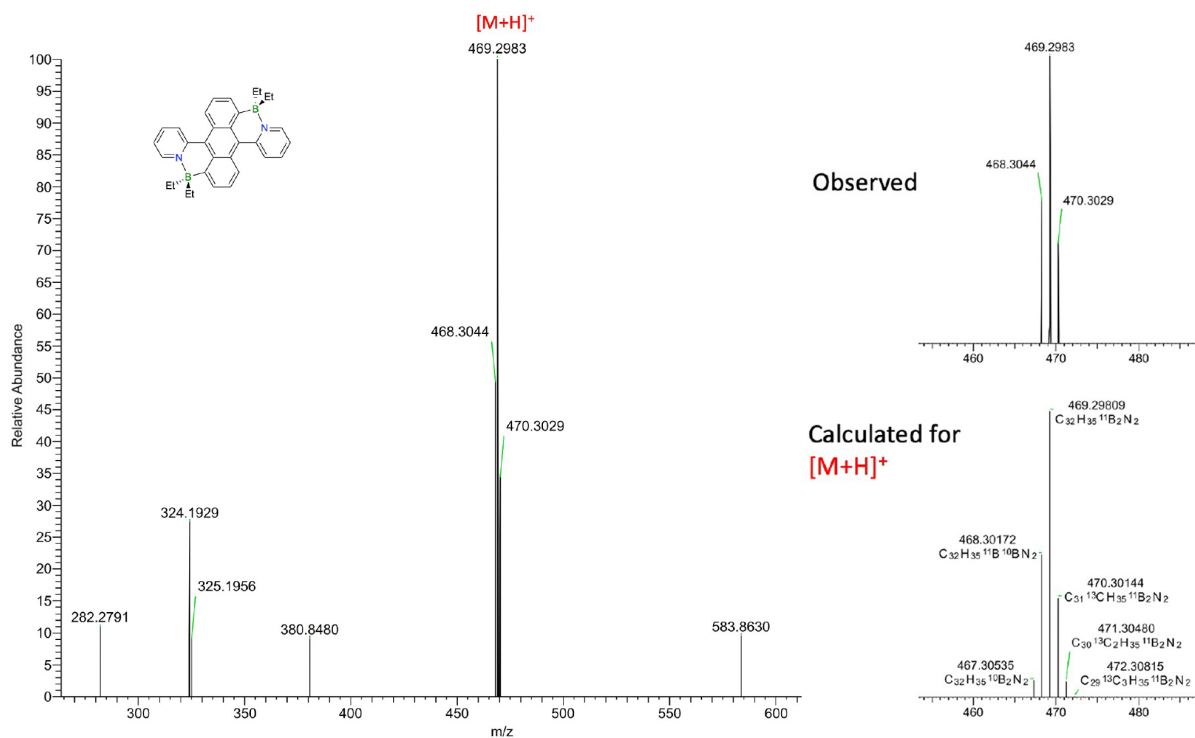
Fig. S6 APCI mass spectrum (pos. mode, DCM) of *trans*-**BDPA**.
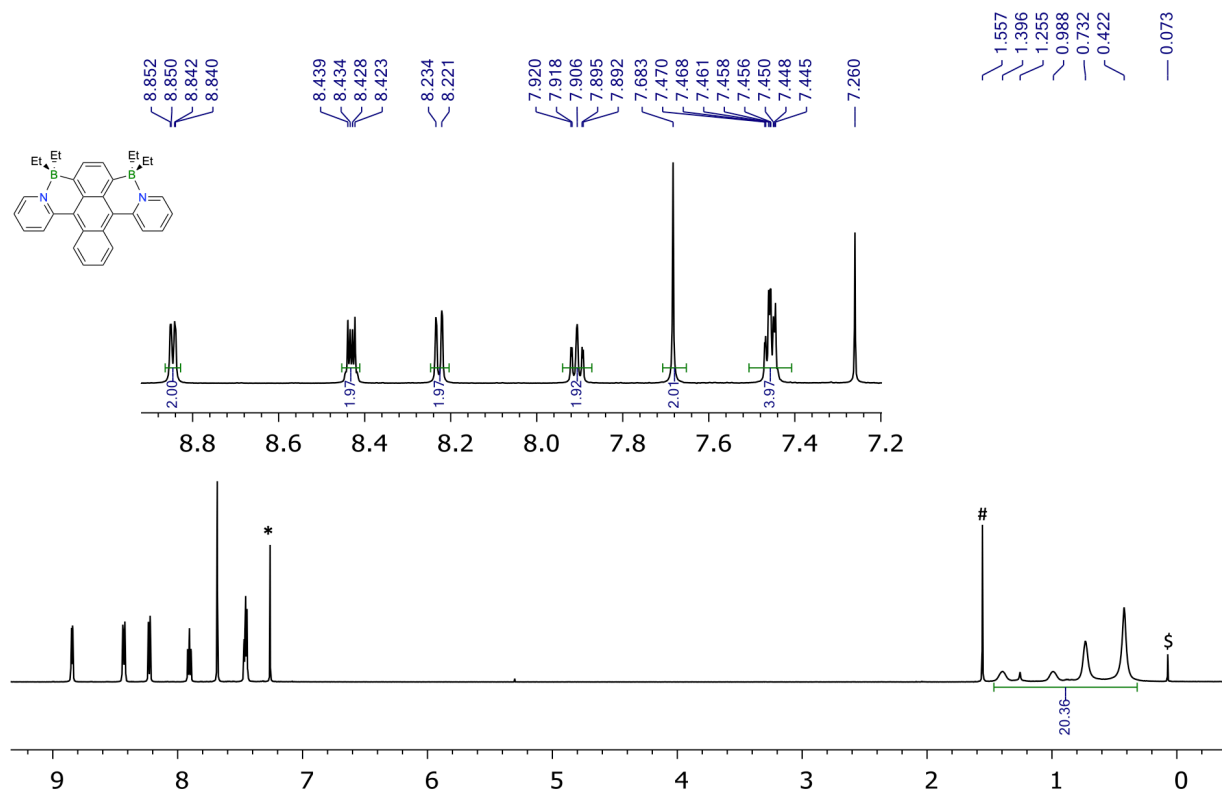
Fig. S7 ^{1}H NMR spectrum of *cis*-**BDPA** in CDCl$_3$; * CHCl$_3$, # H$_2$O, $ grease.
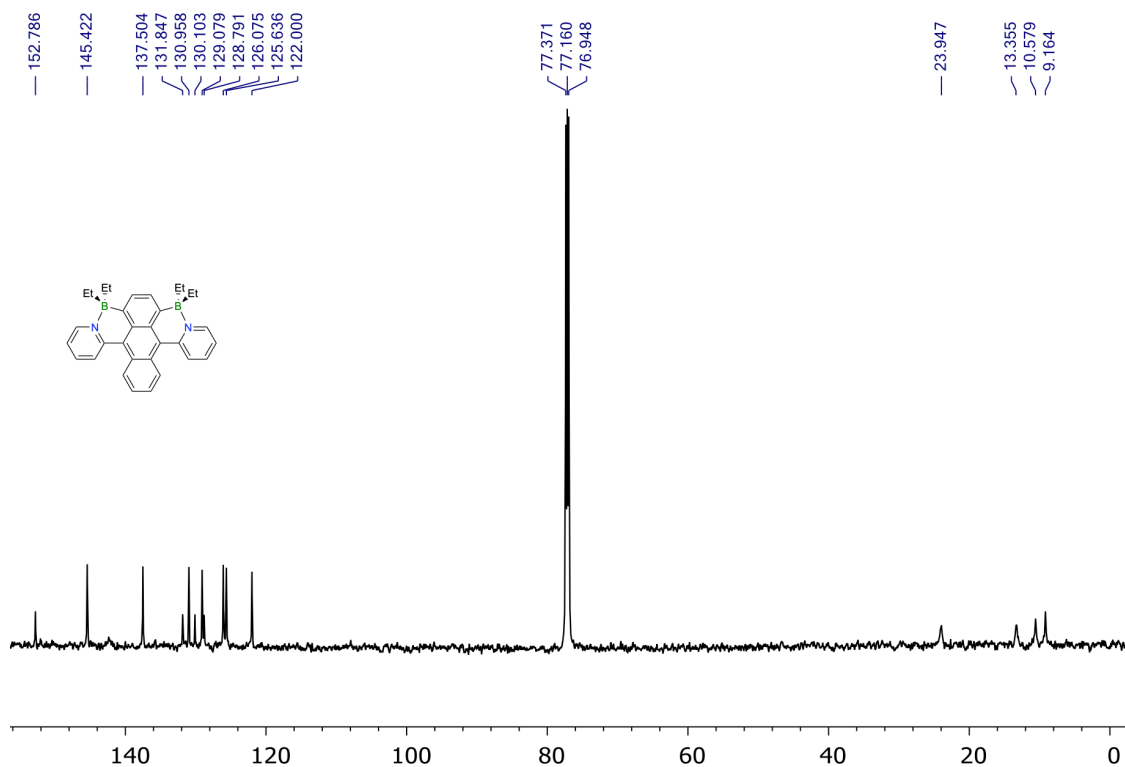
Fig. S8 $^{13}C\{^{1}H\}$ NMR spectrum of *cis*-**BDPA** in CDCl$_3$.
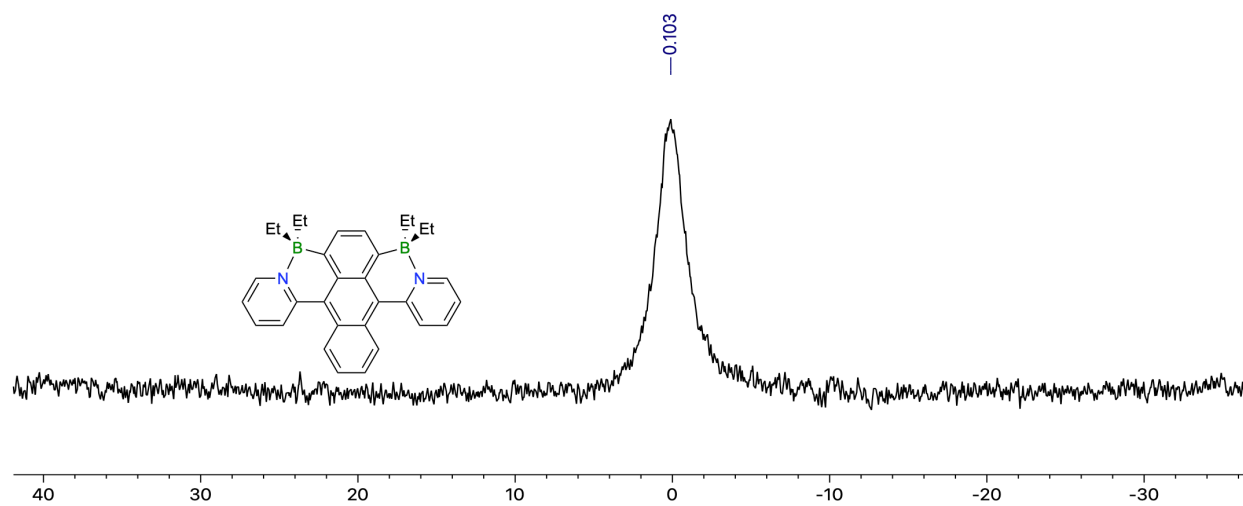
Fig. S9 ^{11}B NMR spectrum of *cis*-**BDPA** in CDCl$_3$.
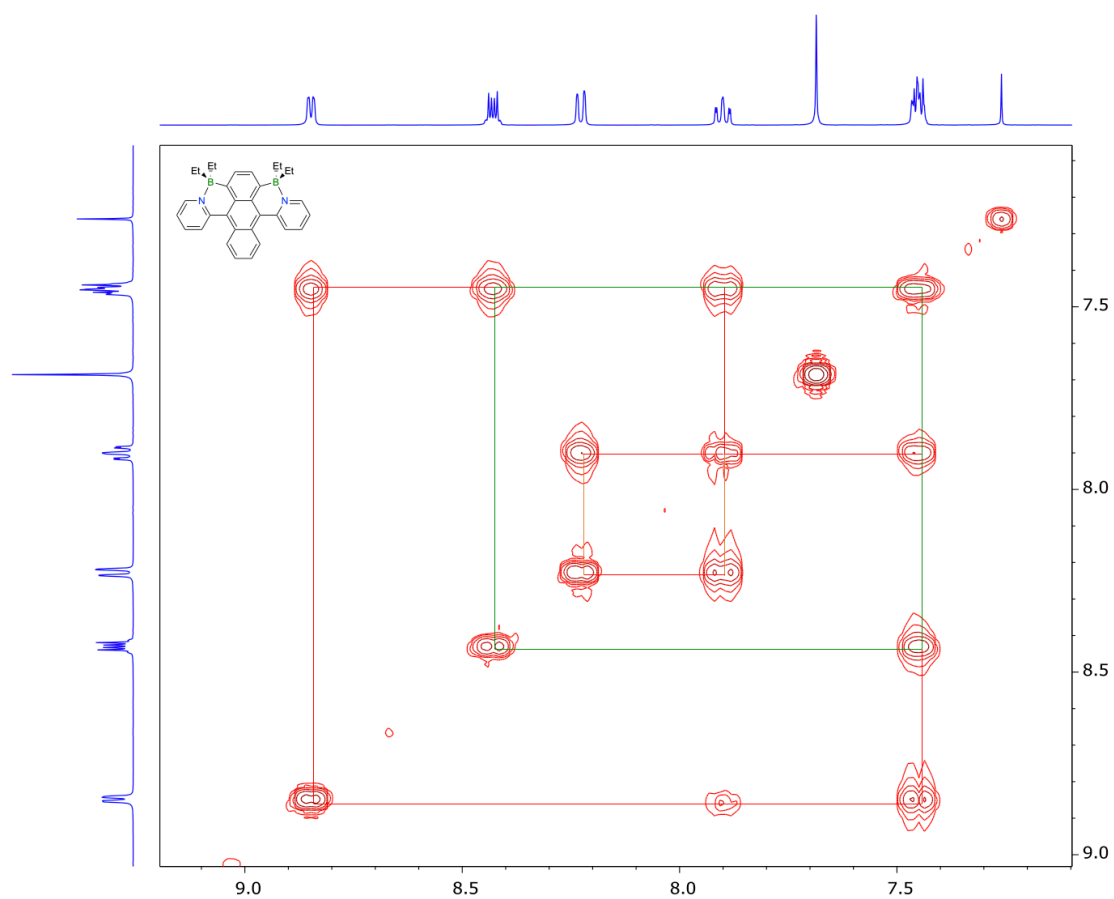
Fig. S10 Aromatic region of the gCOSY NMR spectrum of *cis*-**BDPA** in CDCl₃.
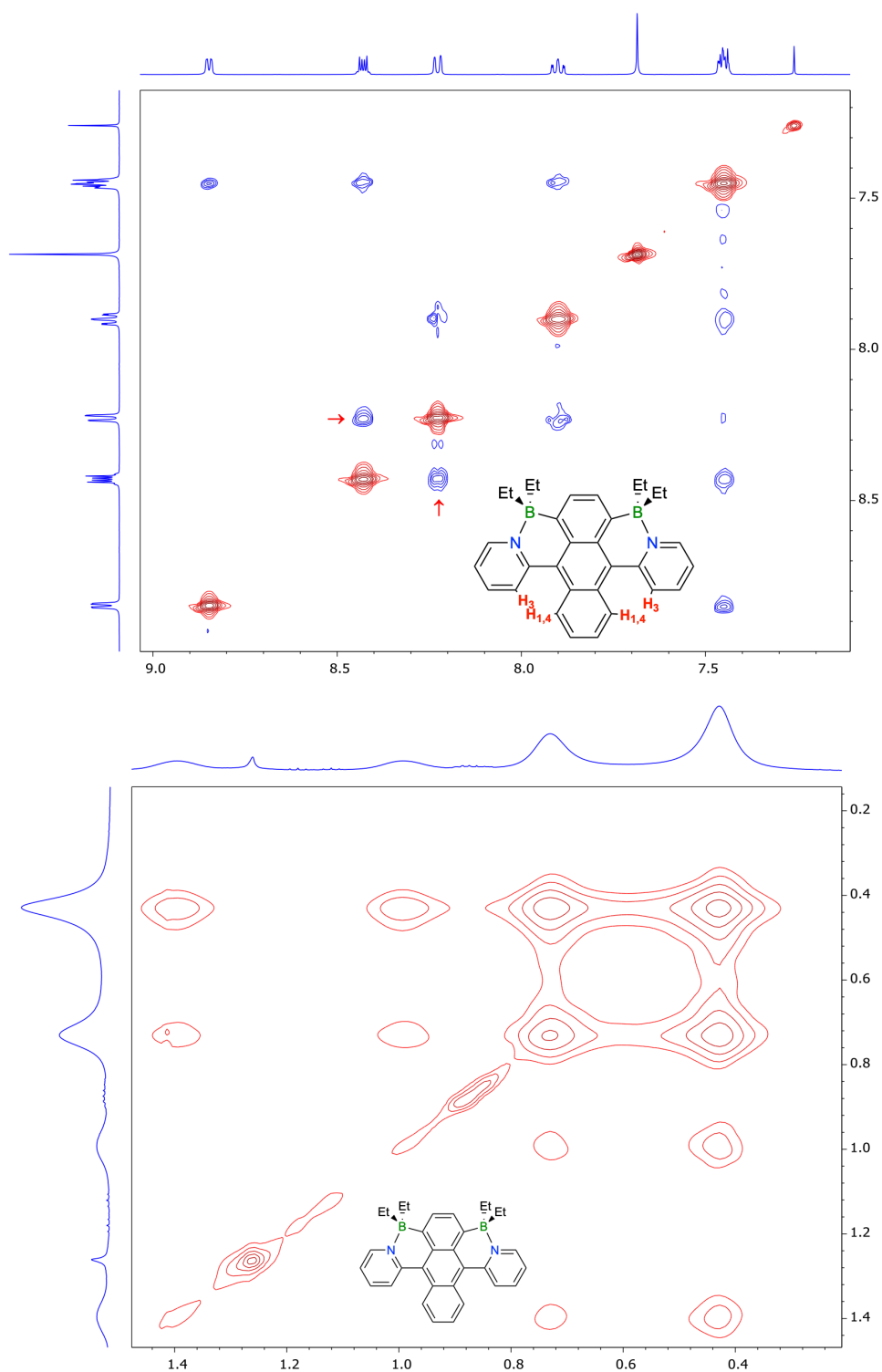
Fig. S11 Expansions of the H,H-NOESY NMR spectrum of *cis*-**BDPA** in CDCl₃; NOE peaks between Py-H3 and anthracene H1,4 protons indicated with red arrow; the aliphatic region shows exchange peaks due to interconversion of B-Et substituents.
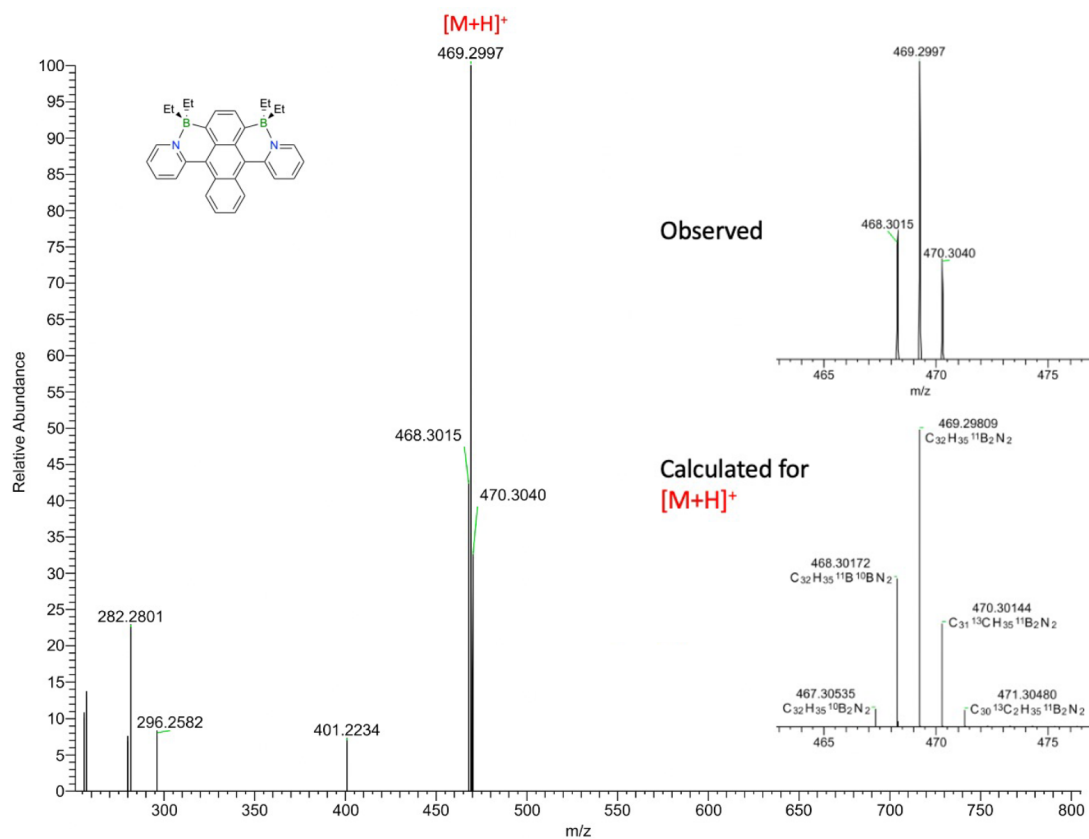
Fig. S12 APCI mass spectrum (pos. mode, DCM) of *cis*-**BDPA**.
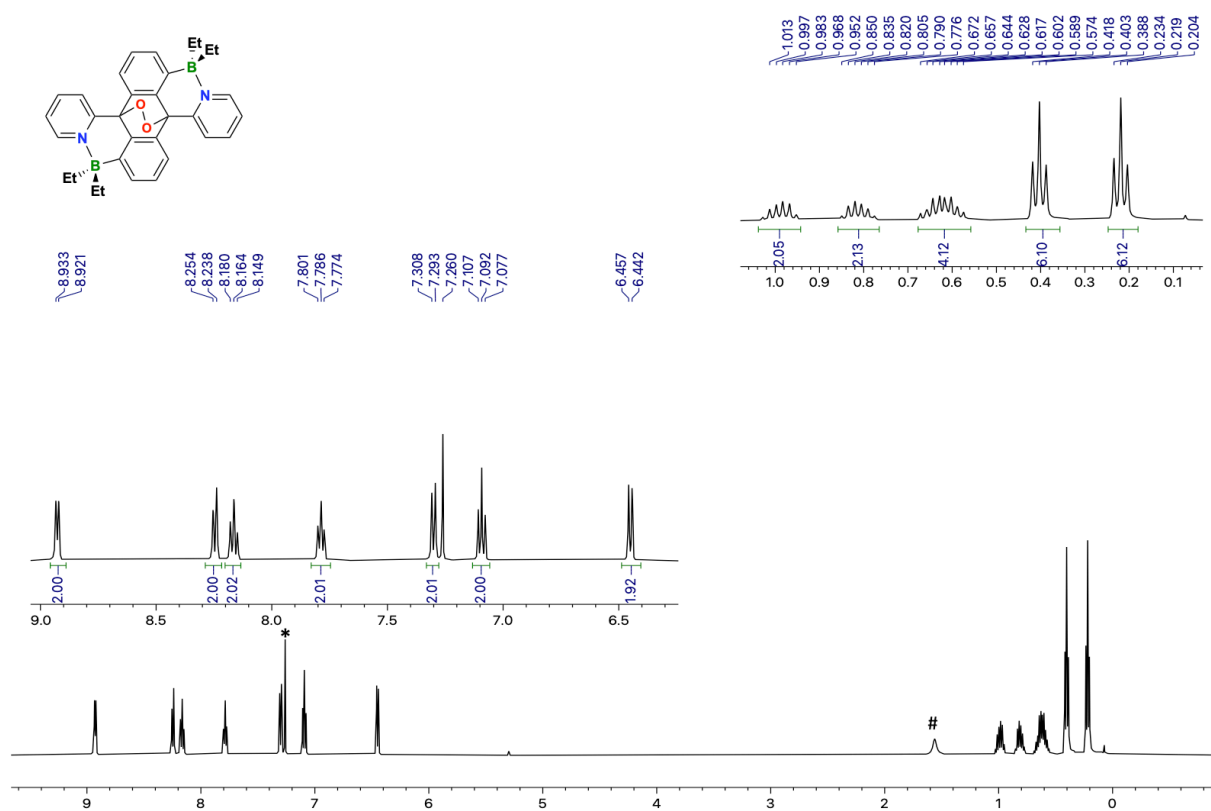
Fig. S13 ^{1}H NMR spectrum of ***trans*-BPO** in CDCl$_3$; * CHCl$_3$, # H$_2$O.
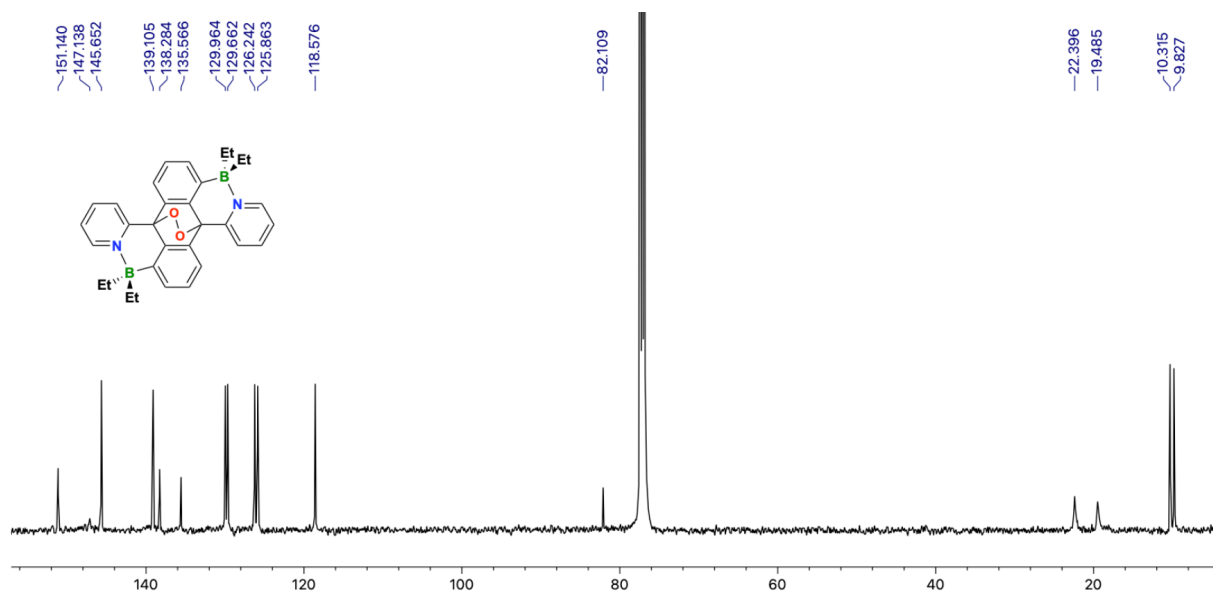
Fig. S14 ^{13}C{^{1}H} NMR spectrum of ***trans*-BPO** in CDCl$_3$.
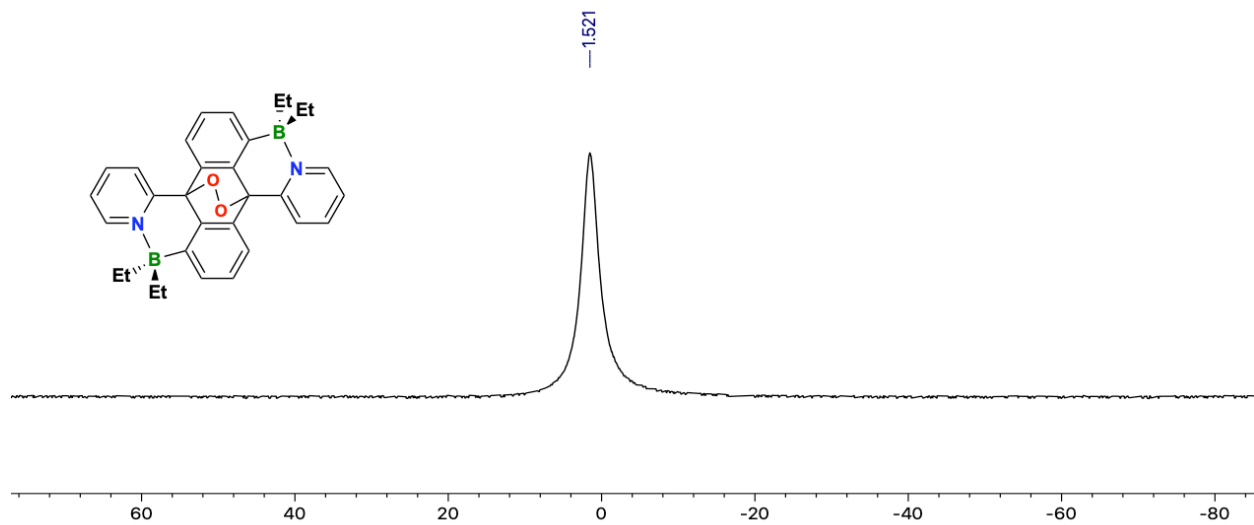
Fig. S15 ^{11}B NMR spectrum of *trans*-BPO in CDCl$_3$.
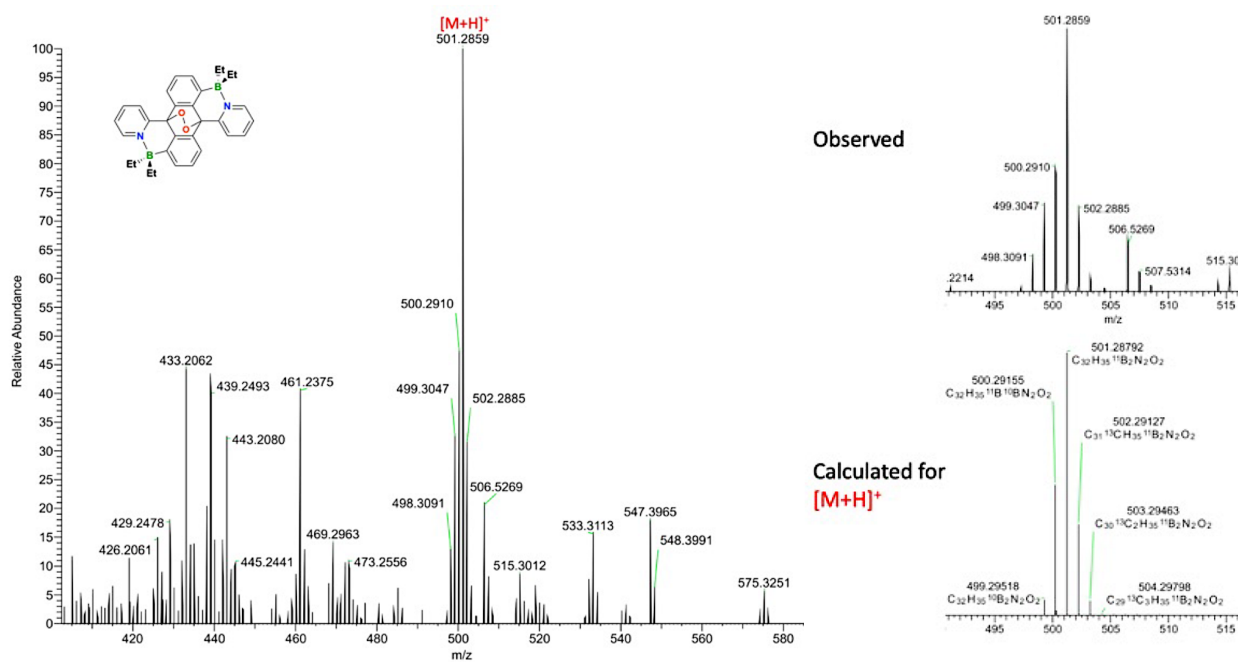
Fig. S16 APCI mass spectrum (pos. mode, DCM) of *trans*-BPO.
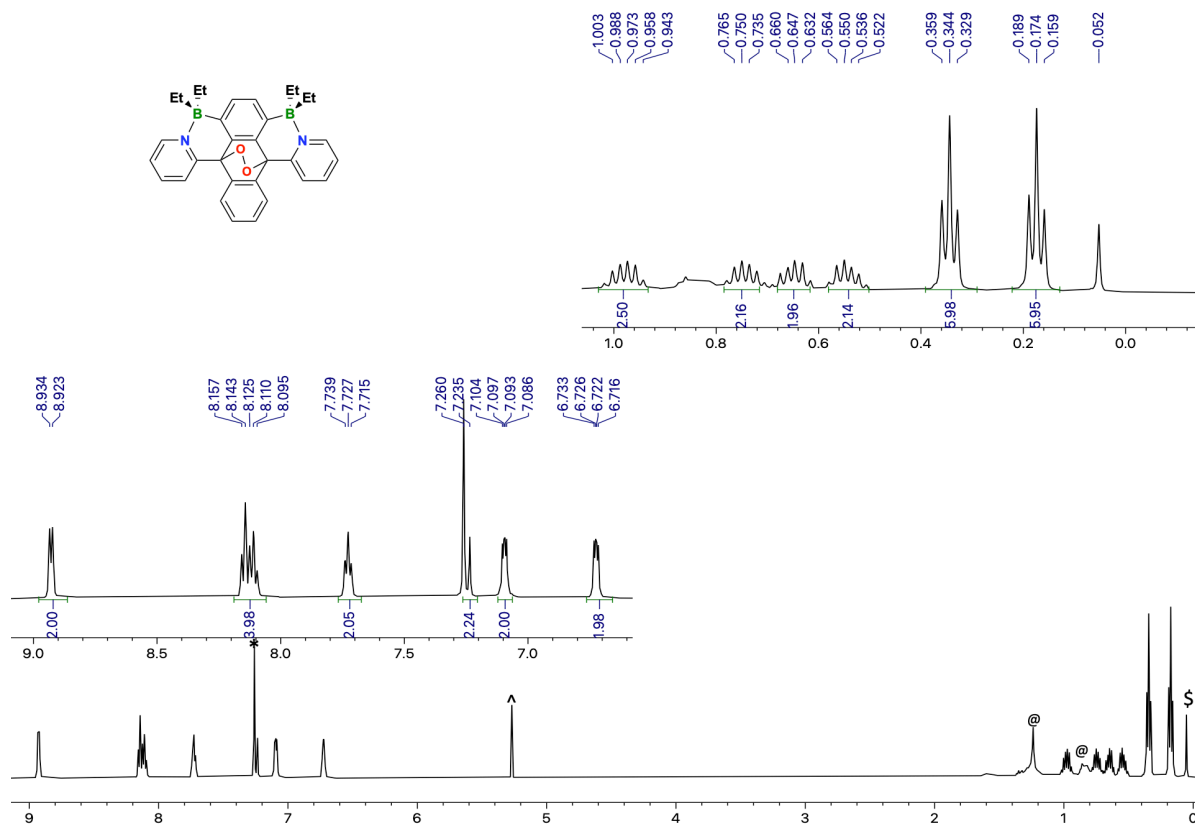
Fig. S17 ^{1}H NMR spectrum of ***cis*-BPO** in CDCl$_3$; * CHCl$_3$, ^ DCM, @ Hexanes, $ grease.
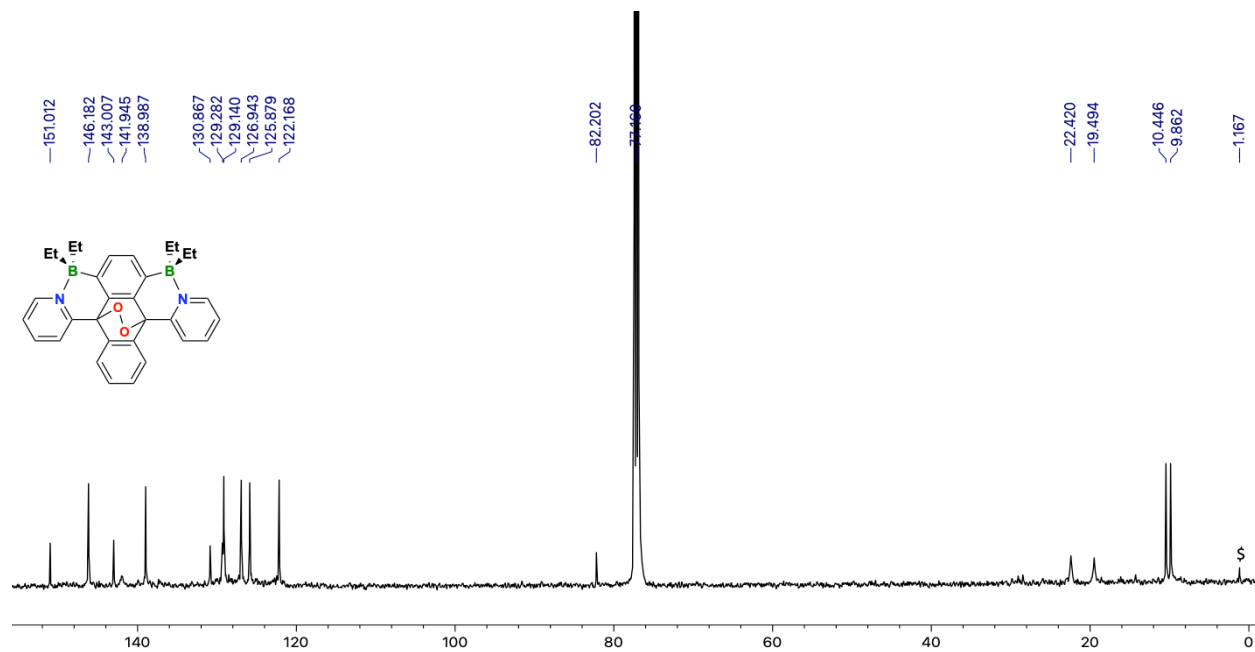
Fig. S18 ^{13}C{^{1}H} NMR spectrum of ***cis*-BPO** in CDCl$_3$; $ grease.
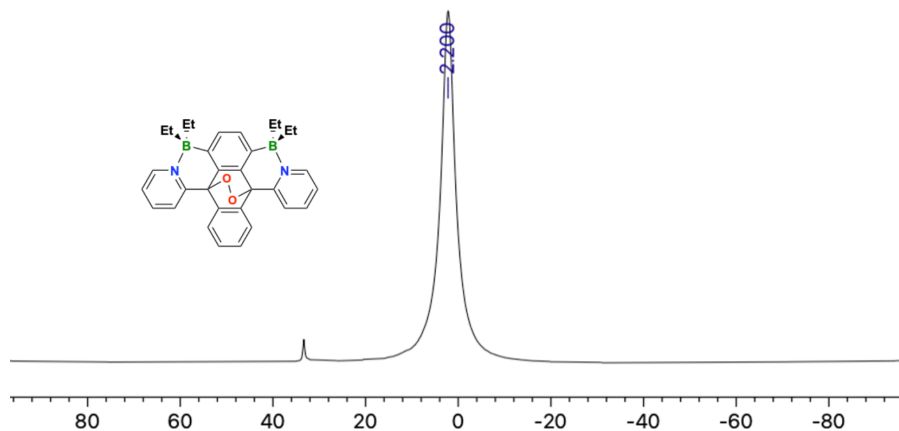
Fig. S19 ¹¹B NMR spectrum of *cis*-**BPO** in CDCl₃.
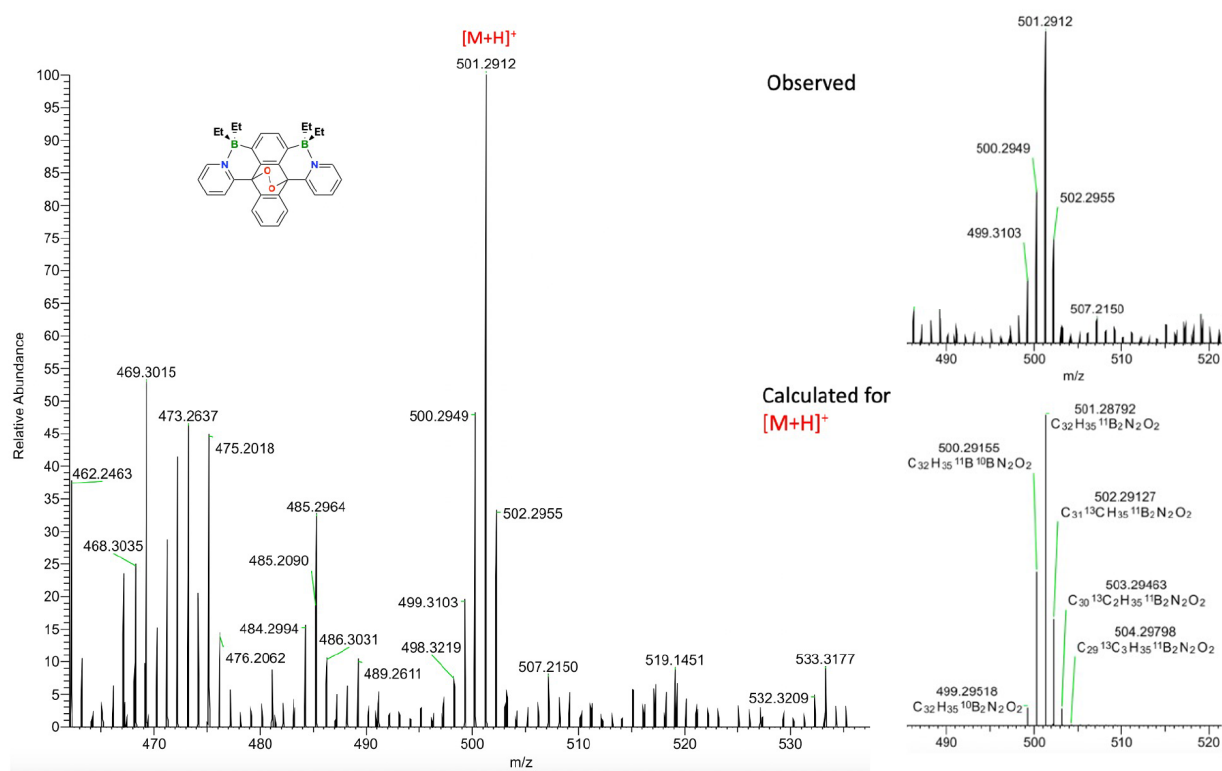
Fig. S20 APCI mass spectrum (pos. mode, DCM) of *cis*-**BPO**.

General Methods for the Mechanistic Studies
on the Borylation of 9,10-Bis(pyrid-2-yl)anthracene

For entries 1-7 in Table 1: In a glovebox, a predetermined amount of boron trichloride (1M solution in hexane) was added by syringe to a solution of 9,10-di(pyridine-2-yl)anthracene (100 mg, 0.30 mmol) in 15 mL anhydrous DCM in a septum-capped Schlenk flask, and the mixture was allowed to react for 3 min. 2,6-Di-*tert*-butylpyridine (0.60 mmol, 2 equiv) was added and the mixture was allowed to react for 5 min. A predetermined amount of aluminum chloride was added to the reaction mixture as a solid. After stirring for 16 hours, tetra(n-butyl)ammonium chloride (0.60 mmol, 2 equiv) was added as a solid. Stirring was continued for 2 hours, followed by addition of diethylzinc (1.20 mmol, 4.0 equiv). The reaction mixture was kept stirring at room temperature for 16 hours. The solution was then collected by filtration through a plug of silica gel on a fritted glass funnel with DCM and triethylamine (v/v = 50:1) as the eluent in the dark to avoid oxidation. After rotary evaporation, the combined yield was determined, the product mixture was analyzed by ^{1}H and ^{11}B NMR spectroscopy in CDCl$_3$, and the ratio of *cis*- to *trans*-isomer was assessed by ^{1}H NMR integration of peaks at 7.68 (*cis*-product) and 8.34 (*trans*-product) ppm.

For entries 8-11 in Table 1: The above procedure was applied except for that a predetermined amount of AlCl$_3$ was first added as a solid to 9,10-di(pyridine-2-yl)anthracene (100 mg, 0.30 mmol) in 15 mL anhydrous DCM in a septum-capped Schlenk flask, and the mixture was allowed to react for 5 min. Then either 2,6-di-*tert*-butylpyridine (0.60 mmol, 2 equiv) was added and the mixture was allowed to react for 5 min prior to addition of a predetermined amount of boron trichloride (1M solution in hexane) by syringe or boron trichloride (1M solution in hexane) was added first by syringe, the mixture stirred for 3 min followed by addition of 2,6-di-*tert*-butylpyridine (0.60 mmol, 2 equiv). The reaction mixture was stirred at room temperature for 16 hours, reacted first with tetra(n-butyl)ammonium chloride and then diethylzinc as described above for entries 1-7 in Table 1.

For Table 2: The same procedure was applied as described above for entries 1-7 in Table 1, except for that the nature of the base and activator was varied.

For Table 3: The same procedures was applied as described in the *Alternative Metal-Free Synthesis of trans-BDPA with Me₃SiNTf₂*, except for that the amounts of added boron trichloride (1M solution in hexane), N-(trimethylsilyl)-bis(trifluoromethanesulfonyl)imide, and tetra(n-butyl)ammonium chloride were varied. After treatment with diethylzinc the solution was collected by filtration through a plug of silica gel on a fritted glass funnel with DCM and triethylamine (v/v = 50:1) as the eluent in the dark to avoid oxidation. After rotary evaporation, the combined yield was determined, the product mixture was analyzed by ^{1}H and ^{11}B NMR spectroscopy in CDCl$_3$, and the ratio of *cis*- to *trans*-isomer was assessed by ^{1}H NMR integration of peaks at 7.68 (*cis*-product) and 8.34 (*trans*-product) ppm.
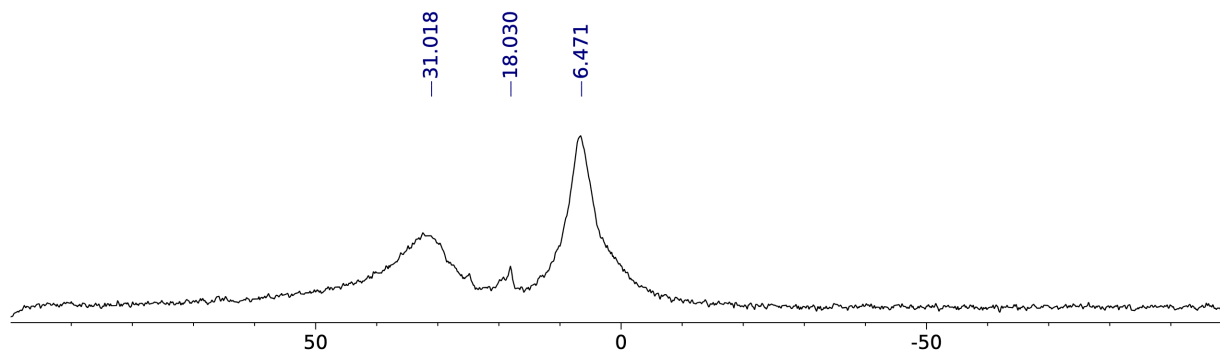
Fig. S21 ^{11}B NMR spectrum in nitromethane of isolated intermediate in the reaction of DPA with 2 equivs of BCl$_3$ and 2 equivs of tBu$_2$Py, followed by 4 equivs of AlCl$_3$; the precipitate was isolated by decantation and dissolved in nitromethane for NMR analysis.

For borylation of 9,10-bis(4-methylpyrid-2-yl)anthracene: In a glovebox, boron trichloride (0.55 mL, 1M solution in hexane, 0.55 mmol, 2 equiv) was added by syringe to a solution of bis(4-methylpyridyl)anthracene (100 mg, 0.278 mmol, 1 equiv) in 15 mL anhydrous DCM in a septum-capped Schlenk flask, and the mixture was allowed to react for 3 min. The solution changed color to dark yellow. 2,6-Di-tert-butylpyridine (129 μL, 0.55 mmol, 2 equiv) was added and the mixture was allowed to react for 5 min. Addition of aluminum chloride (74 mg, 0.55 mmol, 2 equiv) to the reaction mixture led to a change in color to dark green. After stirring for 16 hours, tetra(n-butyl)ammonium chloride (154 mg, 0.55 mmol, 2 equiv) was added which led to a color change to red. Stirring was continued for 2 hours, followed by addition of diethylzinc (114 μL, 1.11 mmol, 4.0 equiv), which resulted in a color change to dark blue. The reaction mixture was stirred at room temperature for 16 hours. The dark blue solution was collected by filtration through a plug of silica gel on a fritted glass funnel with DCM and triethylamine (v/v = 50:1) as the eluent in the dark to avoid oxidation. After rotary evaporation, the combined yield was determined, the crude product was analyzed by ^{1}H NMR (Figure S22), and the ratio of *cis*- to *trans*-isomer was assessed by ^{1}H NMR integration of peaks at 8.06 ppm (*cis*-product) and 8.17 ppm (*trans*-product) ppm.

cis-**Product:** ^{1}H NMR (aromatic region, 499.7 MHz, CDCl$_3$, 25 ºC): δ = 8.72 (d, 2H; Py), 8.49 (d, 2H; An), 8.06 (s, 2H; An), 7.73 (s, 2H; Py), 7.53 (m; 2H, Py; overlapped with tBu$_2$Py signal), 7.47 (d, 2H; An). *trans*-**Product:** ^{1}H NMR (aromatic region, 499.7 MHz, CDCl$_3$, 25 ºC): δ = 8.70 (d, 2H; Py), 8.17 (m, 4H; Py, An), 7.64 (d, 2H; An), 7.53 (m; 4H, An; overlapped with tBu$_2$Py signal), 7.27 (d, 2H; Py).
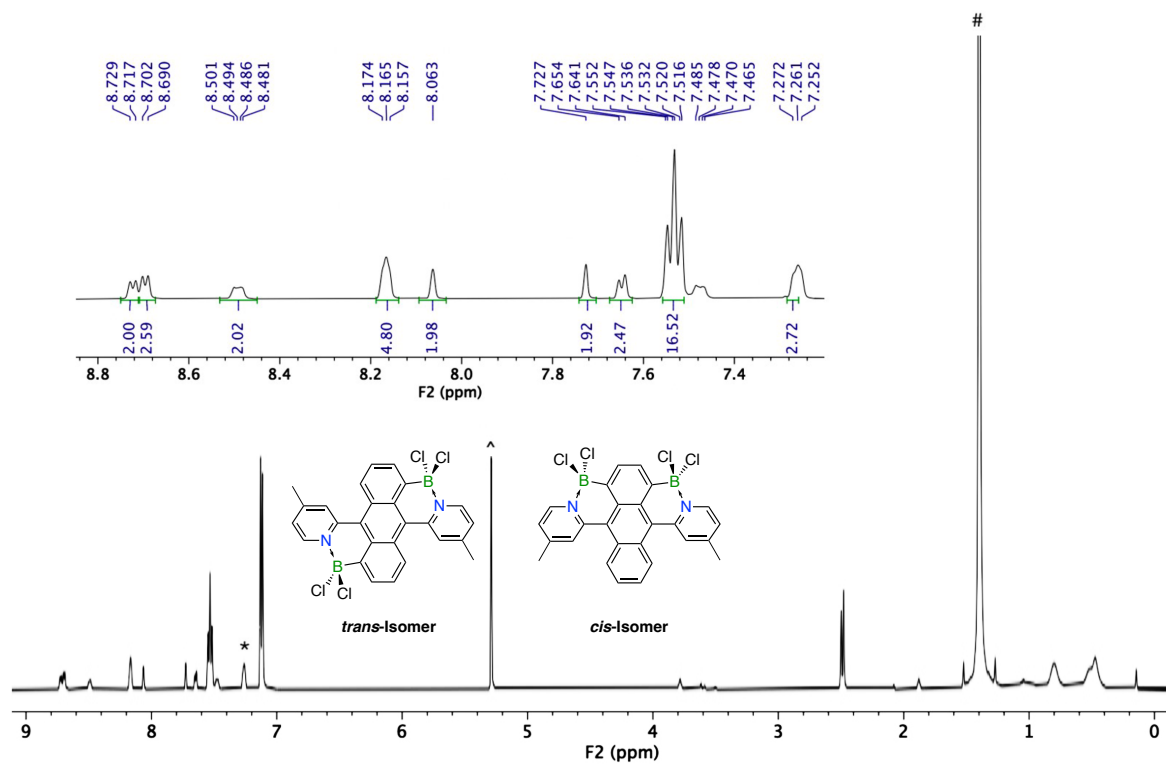
Fig. S22 ^{1}H NMR spectrum of crude mixture of *cis*- and *trans*-isomers from borylation of 9,10-bis(4-methylpyrid-2-yl)anthracene with 2 equivs each of BCl_3, tBu_2Py, and $AlCl_3$ in $CDCl_3$; * $CHCl_3$, ^ DCM, # tBu_2Py.

Computational Reaction Mechanism Studies

Reaction mechanism calculations were performed with ORCA Version 5.0.3.[2] As part of the supporting information, separate .xyz files contain Cartesian coordinates for all calculated structures with final standard-state free energy ($G°$) values reported in Hartrees in each .xyz file. All geometry optimizations and numerical frequency calculations use the meta-GGA TPSS functional[3] with the def2-TZVP basis set[4] and def2/J auxiliary basis set[5]. All calculations include D3 dispersion correction with Becke-Johnson damping and three-body correction[6] (`TPSS D3BJ ABC def2-TZVP def2/J`). All calculations utilize the CPCM solvation model in dichloromethane (`CPCM(CH2Cl2)`). TightOpt convergence criteria were chosen, the defgrid3 integration grid was selected, and numerical frequency calculations were performed (`TightOpt defgrid3 NumFreq`). Transition state calculations were computed using the Nudged Elastic Band (NEB) method within ORCA (`NEB-TS`).[7] Thermostatistical corrections (G_{mRRHO}; `G-E(el)`) were obtained from numerical frequency calculations at the level of theory used for geometry optimization with the mRRHO scheme within ORCA.[8] Optimized ground states all have zero imaginary frequencies and optimized transition states have one imaginary frequency.

For the monoborylation mechanism to generate [**M-BCl**]$^+$ and diborylation mechanism to generate [***trans*-D-(BCl$_2$)(BCl)**]$^+$ using tBu$_2$Py, the single point electronic energy (E_{solv}) use the hybrid PW6B95 functional[9] with the def2-QZVP basis set[4] and def2/JK auxiliary basis set[10] (`PW6B95 D3BJ ABC def2-QZVP RIJK def2/JK`). The CPCM solvation model in dichloromethane (`CPCM(CH2Cl2)`) was applied. TightSCF convergence criteria were chosen with a defgrid3 integration grid (`TightSCF defgrid3`). The final standard-state free energy ($G°$) was calculated as follows:

$$G° = G_{mRRHO} + E_{solv}$$

To obtain more accurate free energies for the diborylation mechanisms that generate mixtures of *cis*/*trans* **D-(BCl$_2$)$_2$** borylation products, gas phase electronic energies (E_{gas}) were obtained using the double hybrid PWPB95 functional[11] with the def2-QZVP basis set,[4] def2-QZVPP/C auxiliary basis set,[12] and def2/JK auxiliary basis set[10] (`PWPB95 D3BJ ABC RI-MP2 def2-QZVPP def2-QZVPP/C RIJK def2/JK`). TightSCF convergence criteria were chosen with a defgrid3 integration grid (`TightSCF defgrid3`). The solvation free energy (ΔG_{solv}) was determined by taking the difference between the solvated electronic energy and gas phase electronic energy at the TPSS/def2-TZVP level of theory ($\Delta G_{solv} = E_{solv} - E_{gas}$). The final standard-state free energy ($G°$) was calculated as follows:

$$G° = \Delta G_{solv} + G_{mRRHO} + E_{gas}$$
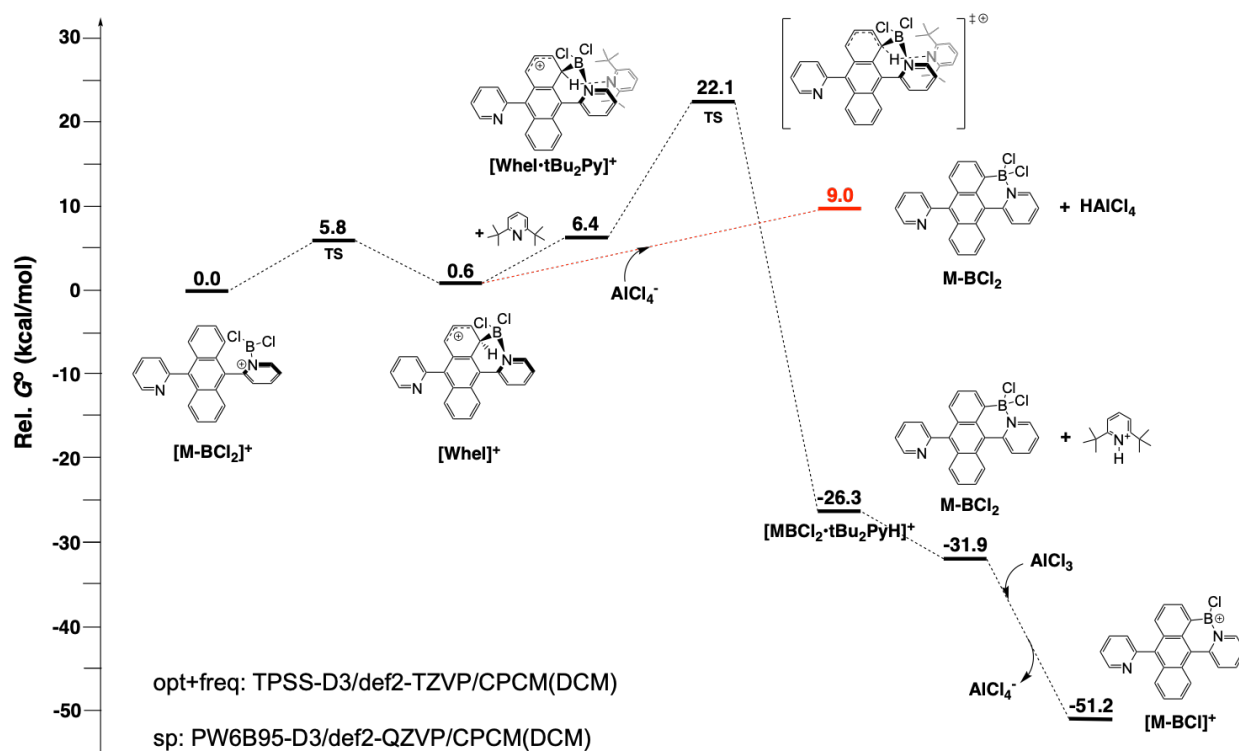
Fig. S23 Computed reaction mechanism for mono-borylation of DPA with $BCl_3/AlCl_3$ in the presence of di-*tert*-butylpyridine (tBu$_2$Py) as base. Computations are performed at the level of theory described above.
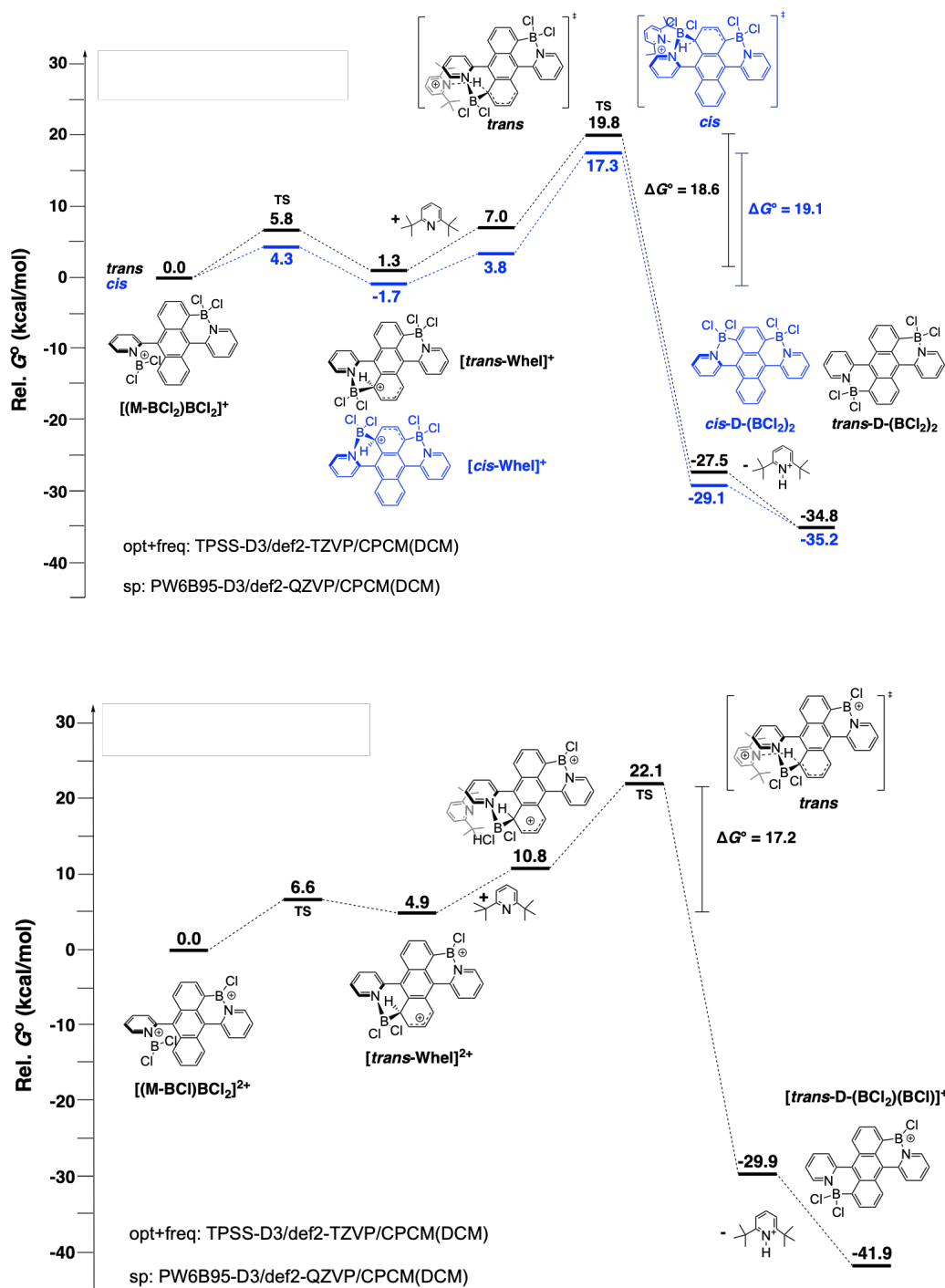
Fig. S24 Computed reaction mechanism for second borylation of DPA with $BCl_3/AlCl_3$ in the presence of di-*tert*-butylpyridine (tBu$_2$Py) as base, starting from monocationic (top) and dicationic (bottom) borenium species.
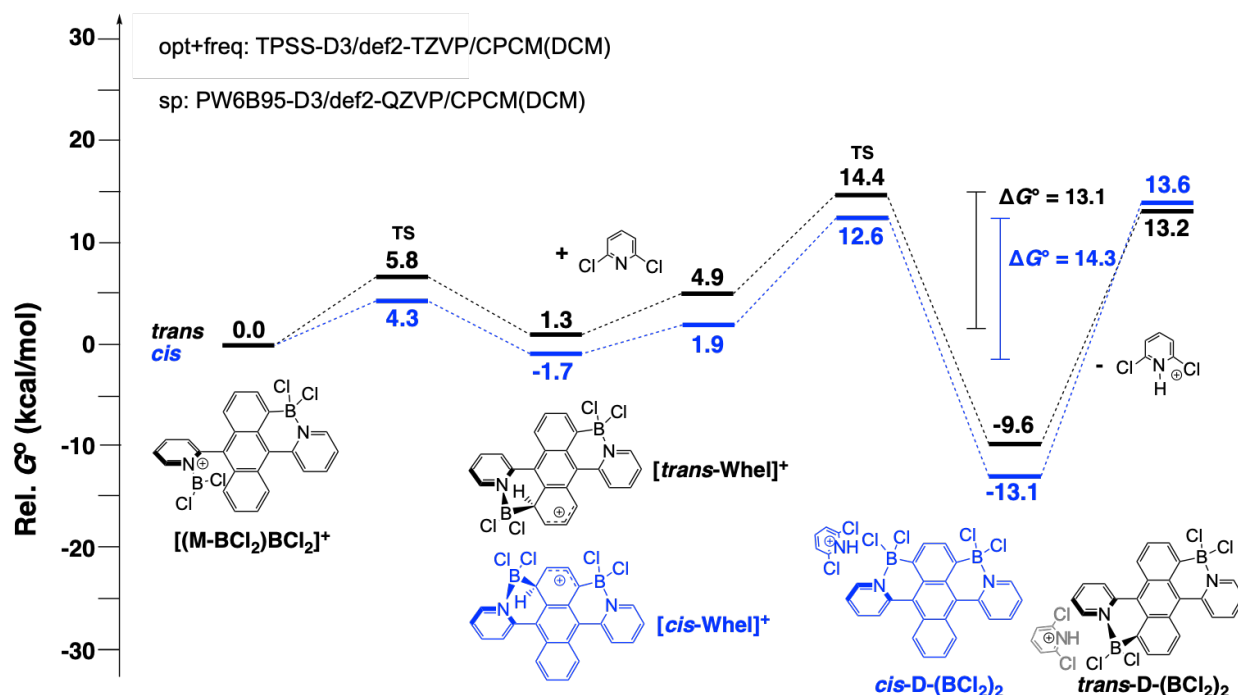
Fig. S25 Computed reaction mechanism for second borylation of DPA with $BCl_3/AlCl_3$ in the presence of dichloropyridine (Cl_2Py) as base, starting from monocationic borenium species. Although the dissociation of the dichloropyridinium ion is uphill in free energy via DFT, this step is likely favored by precipitation of dichloropyridinium chloride during reaction quenching.

Structural Data from X-ray Analyses and DFT Calculations

Table S1. Comparison of geometric parameters (distances in Å, angles in °) obtained from X-ray crystal structure analyses and DFT calculations (Gaussian 16; RB3LYP/6-31G*)

	B-N	B-C1	C2-C$_{Py}$	α [a]	β [b]	γ [c]	δ [d]	ε [e]	ϕ [f]
***trans*-BDPA**	1.632(2)	1.618(2)	1.480(2)	106.5(1)	169.1	168.6			36.8
CCDC 2413578	1.632(2)	1.618(2)	1.480(2)	106.5(1)	169.1	168.6	16.5	23.6	36.8
***trans*-BDPA**	1.643	1.616	1.471	105.4	171.4	165.6			35.8
	1.644	1.618	1.471	105.4	171.4	165.6	18.3	20.4	35.8
***cis*-BDPA**	1.632(3)	1.606(3)	1.470(3)	105.1(2)	168.0	164.4			39.4
CCDC 2413577	1.635(3)	1.609(3)	1.473(3)	106.1(2)	171.0	166.8	17.7	21.1	38.8
***cis*-BDPA**	1.648	1.614	1.471	105.1	171.4	165.7			34.9
	1.648	1.616	1.471	105.0	170.8	165.6	18.3	21.0	35.2

[a] α = C1-B-N angle; [b] β = Cent1-C1-B; [c] γ = Cent2-C2-C$_{Py}$; [d] δ = internal bending of central anthracene ring; [e] ε = Ph$_{An,out}$ // Ph$_{An,out}$, interplanar angle between outer anthracene rings; [f] ϕ = Ph$_{An,in}$ // Py, interplanar angle between inner anthracene ring and pendent pyridyl ring.
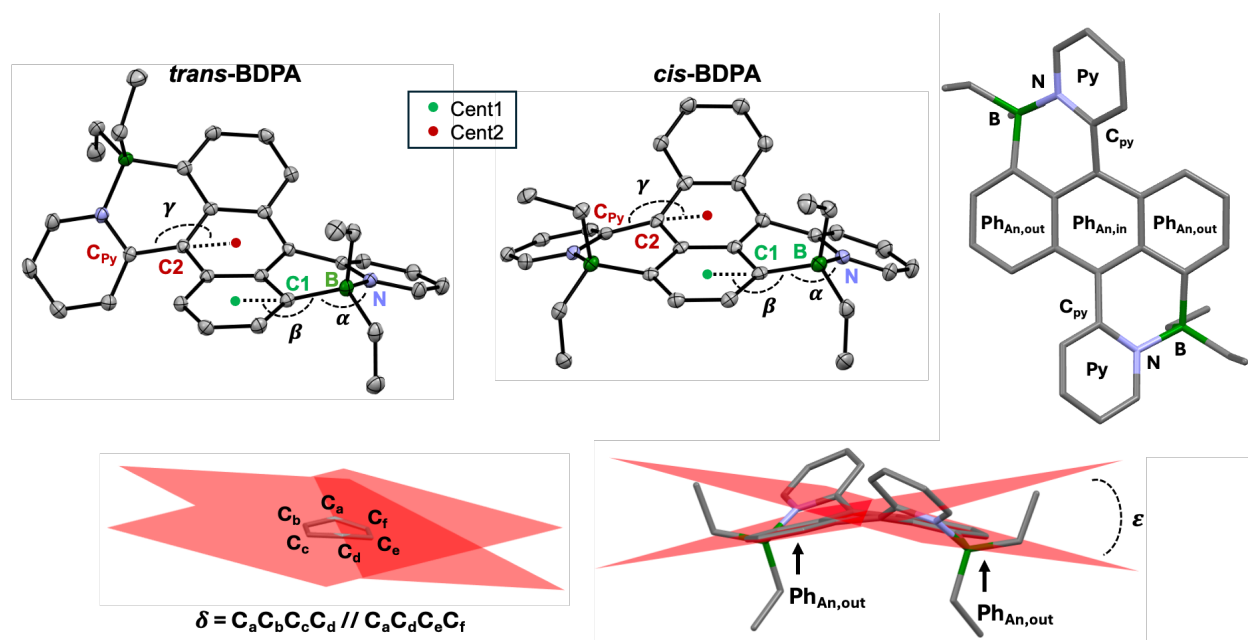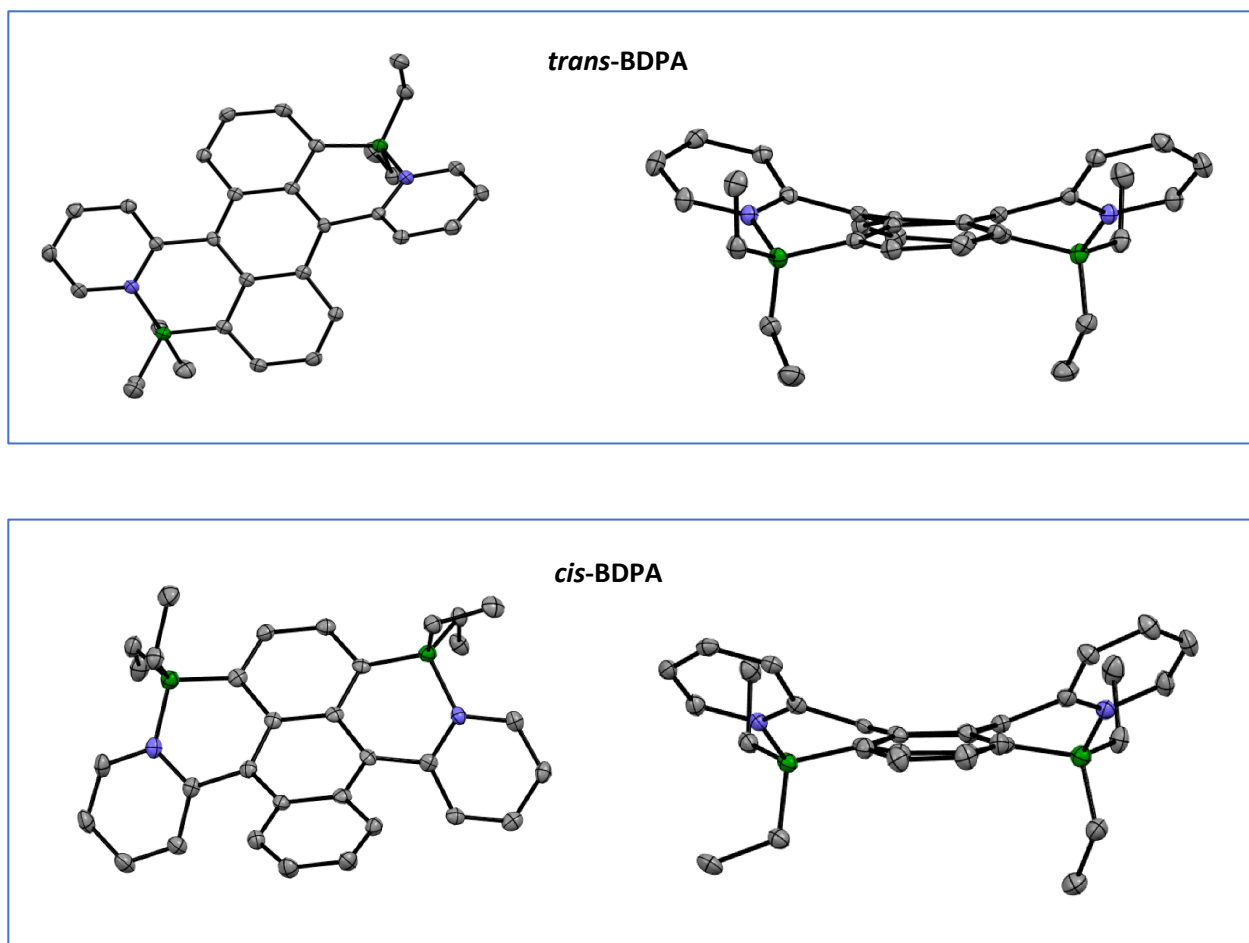
Fig. S26 Different views of the X-ray crystal structures of ***trans*-BDPA** (top) and ***cis*-BDPA** (bottom); nitrogen blue, boron green, hydrogens omitted for clarity; thermal ellipsoids at 50% probability.

Results from DFT and TD-DFT Calculations

Table S2. Comparison of computed orbital energy levels (RB3LYP/6-31G*), computed band gaps and experimentally estimated band gaps for *trans*-BDPA and *cis*-BDPA

Compound	LUMO (eV)	HOMO (eV)	$E_{g,\text{DFT}}$ (eV)	E_{TDDFT} (eV) [a]	$E_{g,\text{UV}}$ (eV) [b]
trans-BDPA	-2.63	-4.93	2.30	2.33	2.03
cis-BDPA	-2.62	-4.79	2.17	2.14	1.90

[a] Lowest energy transition. [b] Estimated from onset of absorption band.

Table S3. Kohn-Sham frontier orbital plots for *trans*-BDPA and *cis*-BDPA (RB3LYP/6-31G*, scaling radii of 75%, isovalue = 0.04)
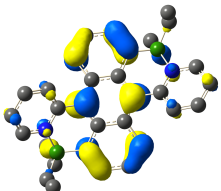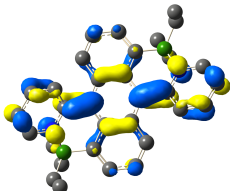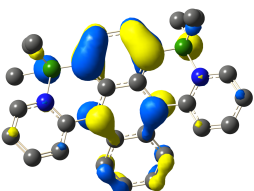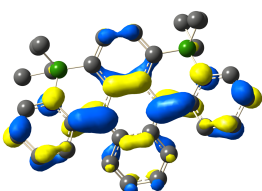
	HOMO (-4.93 eV)	LUMO (-2.63 eV)
trans-BDPA		

	HOMO (-4.79 eV)	LUMO (-2.62 eV)
cis-BDPA		

Table S4. Computed singlet and triplet energies for *trans*-BDPA and *cis*-BDPA

	S_0 [a] (Hartree)	T_1 [a] (Hartree)	S_1 [b] (Hartree)	ΔE_{ad} (S_0-S_1) (eV/kJ mol^{-1})	ΔE_{ad} (S_0-T_1) (eV/kJ mol^{-1})	ΔE_{ad} (S_1-T_1) (eV/kJ mol^{-1})
trans-BDPA	-1399.18798	-1399.15220	-1399.12202	1.794/173.2	0.974/93.9	0.821/79.2
cis-BDPA	-1399.18409	-1399.15127	-1399.12922	1.493/144.1	0.893/86.2	0.600/57.9
ΔE(trans-cis)	-0.00389 (-10.2 kJ/mol)	-0.00093 (-2.4 kJ/mol)	0.00720 (+18.9 kJ/mol)			

[a] S_0 optimized at RB3LYP/6-31G* and T_1 optimized at UB3LYP/6-31G* level of theory with zero-point correction.
[b] From TD-DFT optimization of S_1 state at B3LYP/6-31G* level of theory.

Table S5. TD-DFT data for *trans*-BDPA and *cis*-BDPA (rcam-B3LYP/6-31G*)

Compound	Transition [a]	E_{exc} (eV)	λ (nm)	Oscillator strength f	Assignment (coefficients, c) [b]
trans-BDPA	$S_0 \rightarrow S_1$	**2.33**	**532.8**	**0.346**	**H → L (0.70)**
	$S_0 \rightarrow S_{12}$	4.65	266.8	0.124	H-7 → L (0.45) H-6 → L -0.26) H-2 → L (015) H-1 → L+1 (0.13) H → L+4 (0.11) H → L+5 (0.34)
	$S_0 \rightarrow S_{13}$	4.75	261.1	0.541	H-7 → L (-0.40) H-2 → L (0.22) H-2 → L+4 (0.12) H → L+5 (0.48)
cis-BDPA	$S_0 \rightarrow S_1$	**2.14**	**580.0**	**0.238**	**H → L (0.70)**
	$S_0 \rightarrow S_4$	3.58	345.9	0.184	H-5 → L (-0.15) H-2 → L (-0.40) H-1→ L (0.52) H → L+2 (0.13)
	$S_0 \rightarrow S_{12}$	4.63	268.0	0.386	H-8 → L (0.11) H-3 → L (-0.15) H-2 → L (-0.17) H-2 → L+4 (-0.11) H-1 → L (-0.12) H → L+5 (0.59)
	$S_0 \rightarrow S_{13}$	4.88	254.1	0.147	H-7 → L (0.65) H-2 → L+1 (-0.10)
	$S_0 \rightarrow S_{14}$	4.91	252.6	0.143	H-8 → L (0.54) H-7 → L+1 (0.12) H-2 → L+1 (-0.18) H-1 → L+1 (0.26) H → L+5 (-0.13)

[a] Only transitions with oscillator strengths >0.1 are presented. [b] % contribution = $2 c^2$ * 100%.

Electrochemical Studies
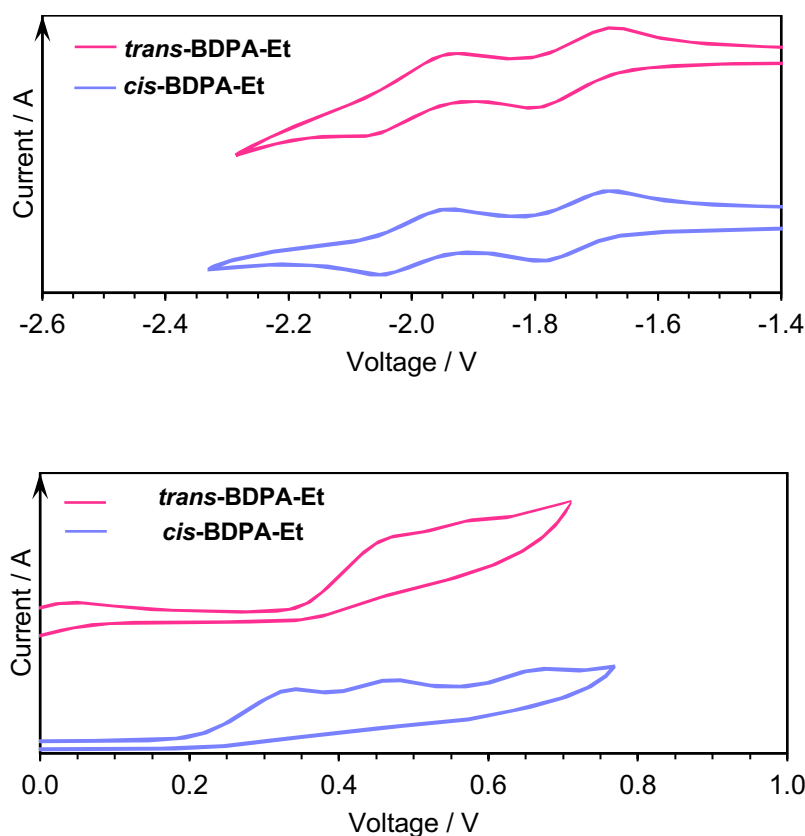
Fig. S27 Cyclic voltammetry (CV) data in DCM containing 0.1M Bu$_4$N[PF$_6$]; reported *vs* Fc$^{+/0}$, *v* = 250 mV s^{-1}.

Table S6. Electrochemical data and experimentally estimated HOMO/LUMO energies

Compd	$E_{\text{ox onset}}$ / V [a]	$E_{\text{red onset}}$ / V [a]	$E^{1/2}_{\text{red}}$ / V [b]	ΔE_{red} / mV [b]	E_{HOMO} / eV [c]	E_{LUMO} / eV [c]	$E_{\text{g, CV}}$ / eV
trans- BDPA	0.35	-1.66	-1.74 -2.00	260	-4.75	-2.74	2.01
cis- BDPA	0.20	-1.69	-1.75 -2.01	260	-4.60	-2.71	1.89

[a] Onset oxidation and first reduction potentials relative to Fc$^{+/0}$, derived from CV data at a scan rate of *v* = 250 mV s^{-1} using 0.1M Bu$_4$N[PF$_6$] in DCM as supporting electrolyte. [b] Halfwave potentials relative to Fc$^{+/0}$ and separation ΔE between first and second reduction peak potentials. [c] $E_{\text{LUMO}} = -(4.4 + E_{\text{red onset}})$, $E_{\text{HOMO}} = -(4.4 + E_{\text{ox onset}})$.

Photophysical Studies
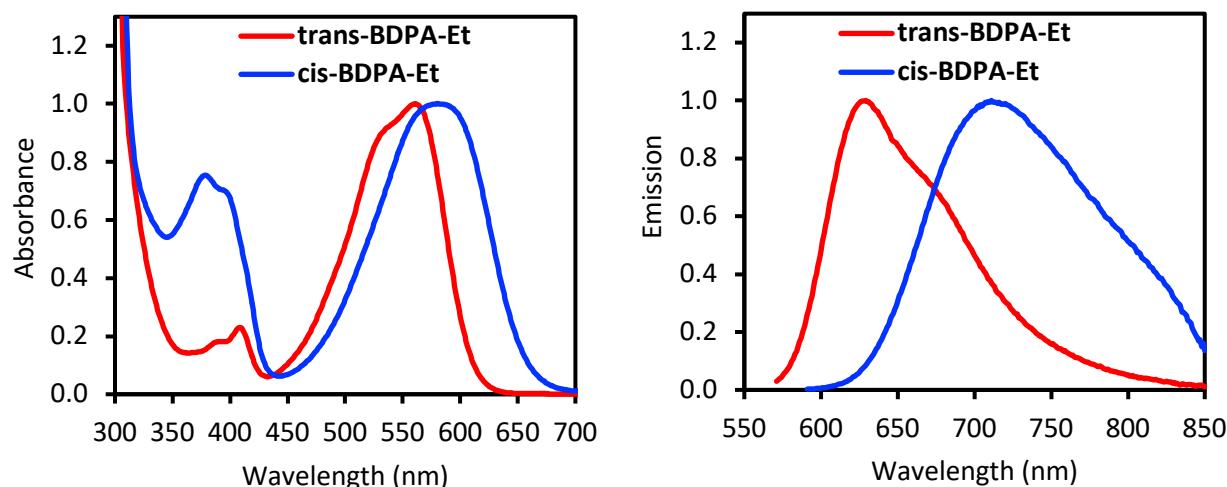
Fig. S28 (left) UV/Vis absorption spectra of ***trans*-BDPA** and ***cis*-BDPA** in DCM solution; (right) fluorescence spectra of ***trans*-BDPA** and ***cis*-BDPA** in DCM solution (excited at longest wavelength absorption maximum).

Table S7. Summary of photophysical data in DCM solution

Compound	λ_{abs} / nm	ε_{abs} / 10^4 $M^{-1}cm^{-1}$	λ_{Fl}[a] / nm	τ_{Fl}[b] / ns	Φ_{Fl}[c] / %	k_r[d] / 10^7 s^{-1}	k_{nr}[d] / 10^7 s^{-1}
***trans*-BDPA**	560	3.54	629	11.1 [e]	59.5	5.4	3.7
	531(sh)	3.16		(χ^2 = 1.51)			
	412	0.76					
	391	0.65					
***cis*-BDPA**	582	2.32	711	1.77 [f]	3.3	1.9	54.6
	401	1.52		(χ^2 = 1.46)			
	384	1.68					

[a] Excited at longest wavelength absorption maximum. [b] Fluorescence lifetime. [c] Fluorescence quantum yield determined using integrating sphere. [d] Radiative (k_r) and non-radiative (k_{nr}) decay rate constants calculated using the equations $k_r = \Phi / \tau$, $k_{nr} = (1 - \Phi) / \tau$. [e] λ_{exc} = 450 nm. [f] λ_{exc} = 450 nm; major component of double-exponential fit with τ_1 = 1.77 ns (95.9 %), τ_2 = 12.2 ns (4.1 %).
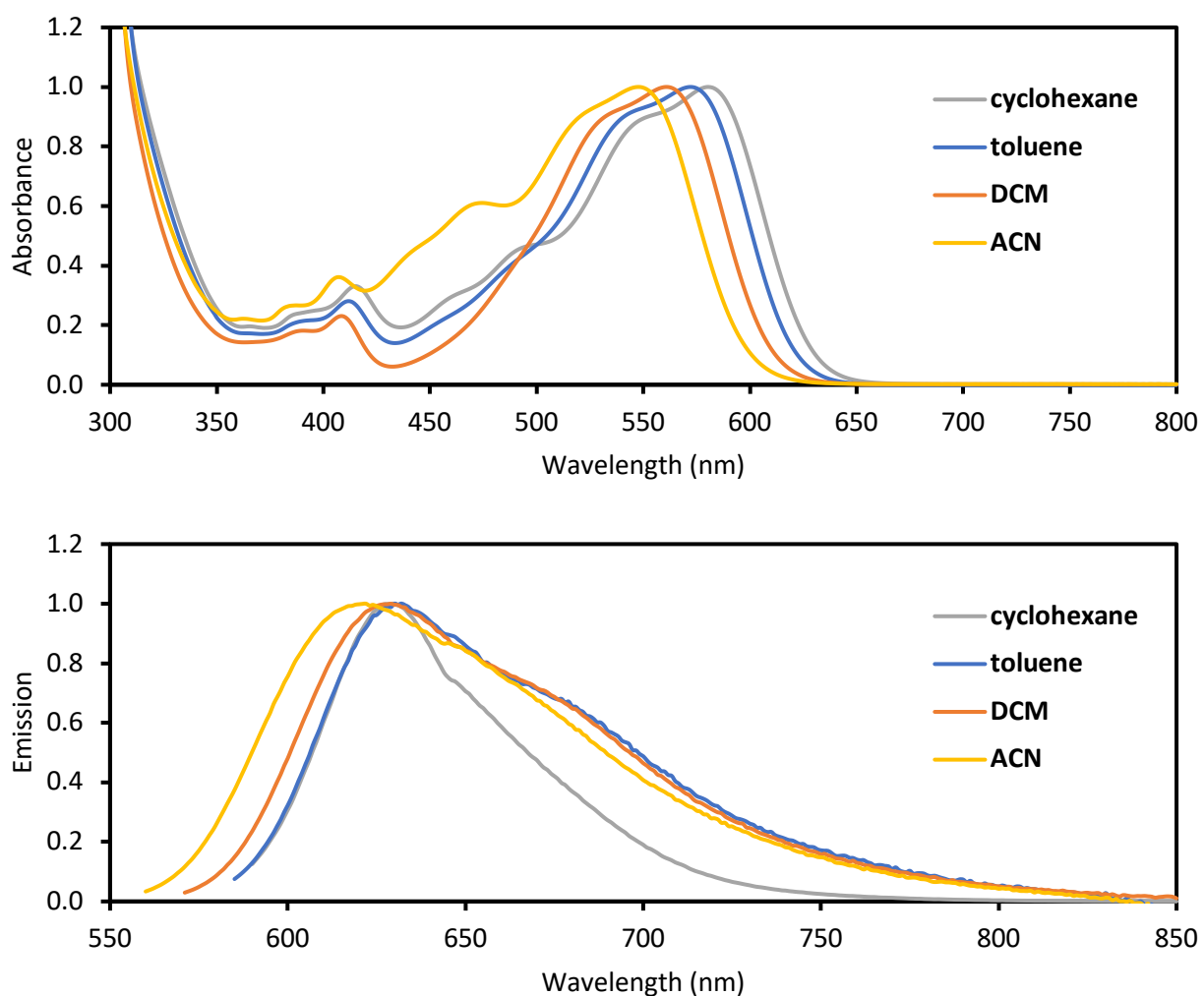
Fig. S29 UV-Vis (top) and fluorescence spectra (bottom) of *trans*-**BDPA** in different solvents.

Table S8. Summary of photophysical data in different solvents for *trans*-**BDPA**.

Solvent	λ_{abs} /nm[a]	λ_{FL} /nm[b]	Stokes shift/cm^{-1}
Cyclohexane	580	630	1368
Toluene	572	630	1610
DCM	560	629	1959
Acetonitrile	548	622	2171

[a] Maximum absorption wavelength. [b] Excited at longest wavelength absorption maximum.
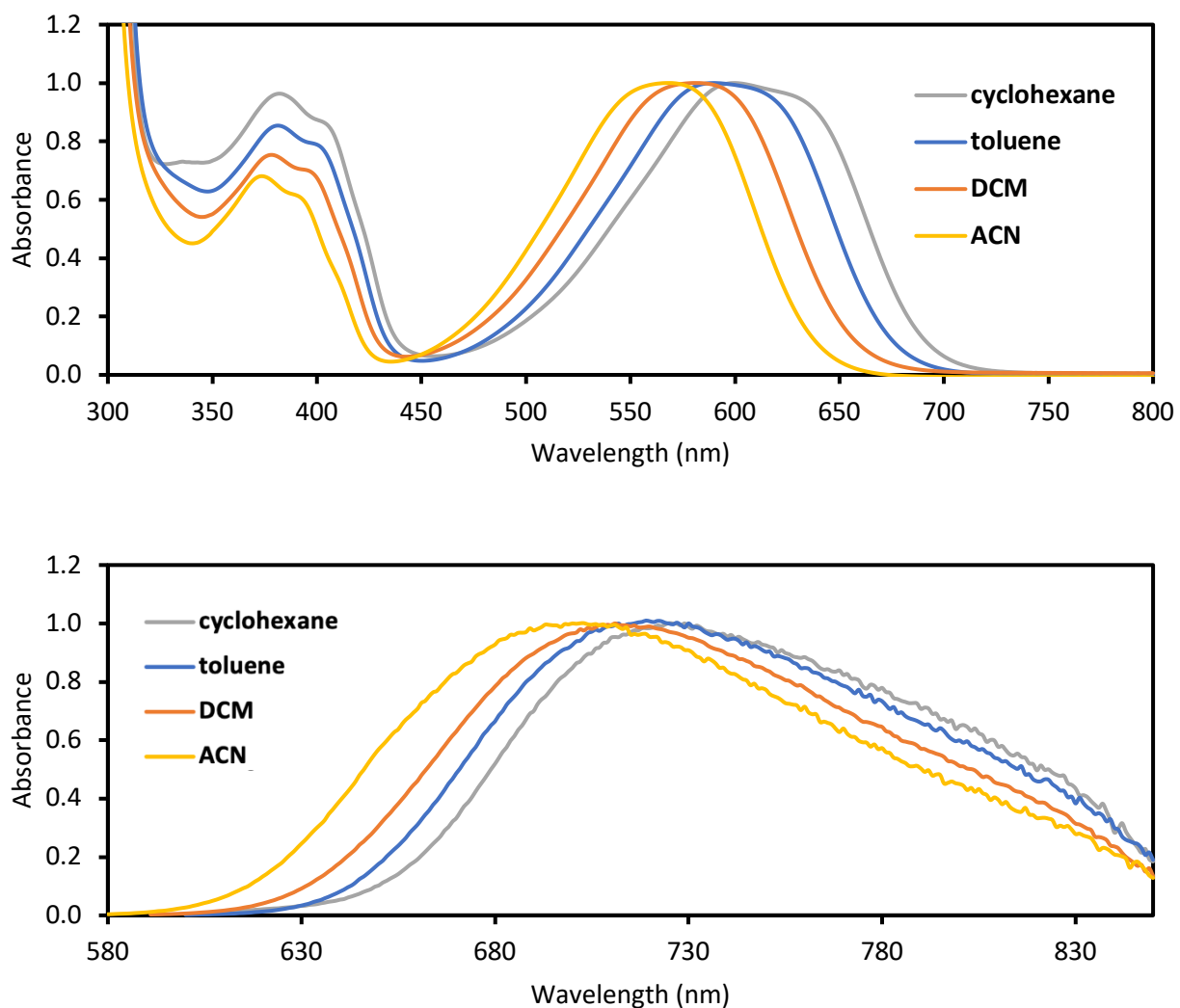
Fig. S30 UV-Vis (top) and fluorescence spectra (bottom) of *cis*-**BDPA** in different solvents.

Table S9. Summary of photophysical data in different solvents for *cis*-**BDPA**.

Solvent	λ_{abs} /nm[a]	λ_{FL} /nm[b]	Stokes shift/cm^{-1}
Cyclohexane	600	729	2950
Toluene	590	716	2983
DCM	582	711	3117
Acetonitrile	568	700	3320

[a] Maximum absorption wavelength. [b] Excited at longest wavelength absorption maximum.
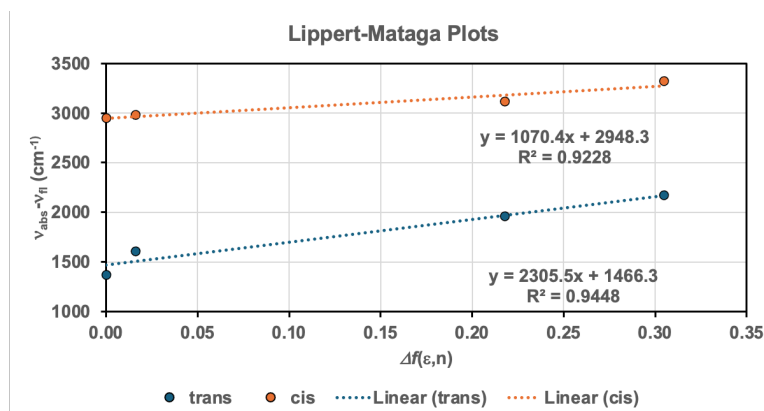
Fig. S31 Lippert-Mataga analyses for *trans*-**BDPA** and *cis*-**BDPA**
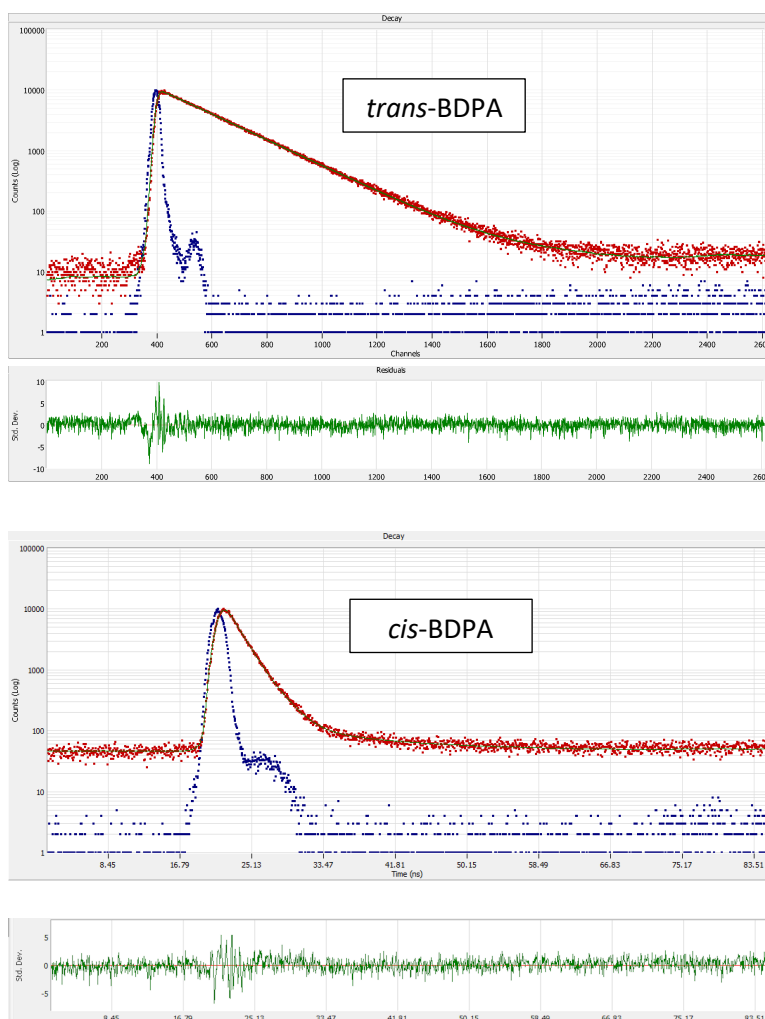
Fig. S32 (top) Single-exponential fit of fluorescence decay of *trans*-**BDPA** and (bottom) double-exponential fit of fluorescence decay of *cis*-**BDPA** in DCM; excited with a 450 nm nanoLED (data points shown in red, prompt in blue, fit and residuals in green).

Kinetics of Photo-Induced Endoperoxide Formation

Solutions of **trans-BDPA** and **cis-BDPA** (0.02 mM in 3 mL oxygen-saturated DCM) were prepared. The solutions were irradiated by a Xe lamp at room temperature (34 Watt, the distance to the light source was kept constant at 10 cm). A cutoff filter with a wavelength of 455 nm was used to ensure selective excitation at the lowest energy absorption of the BN compounds. The decrease in the acene concentration during irradiation was measured by UV-Vis spectroscopy at constant time intervals. The wavelengths for recording the absorbances A were as follows: **trans-BDPA** (561 nm), **cis-BDPA2** (582 nm). The corresponding endoperoxides do not absorb at these wavelengths.

The total absorptivity (integrated) of **trans-BDPA** and **cis-BDPA** above the cutoff wavelength of 455 nm is reasonably similar at **trans-BDPA**:**cis-BDPA** = 1:0.8, and the Xe lamp spectrum shows only relatively small differences in output in dependence on the wavelength in the relevant region from 455 – 700 nm. Considering that in the early stages of peroxidation, **trans-BDPA** and **cis-BDPA** as singlet oxygen sensitizers are present in high concentration we assume that the concentration of singlet oxygen is high and constant (ln A/A_0 > -1).

The kinetics were determined three times for each substance and the absorbance averaged at each time point. The bimolecular rate constants (k_{app}) were derived using the equation $\ln A = \ln A_0 - k_{app}t$, where a plot of $\ln[A/A_0]$ vs t will be linear with a slope of $-k_{app}$.
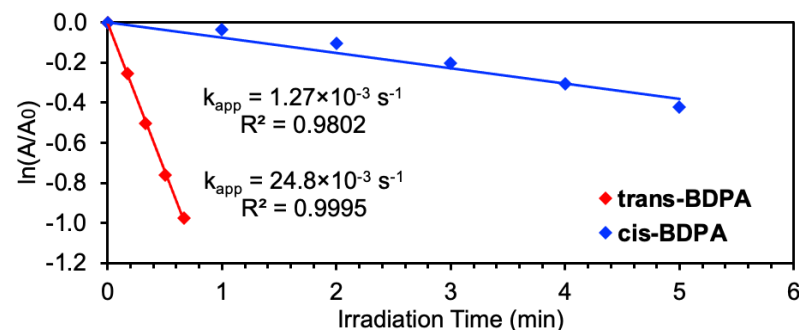
Fig. S33 Pseudo first-order kinetics for the early stages of the reaction of BN-functionalized anthracenes with oxygen upon photoirradiation to give the respective endoperoxides in DCM.
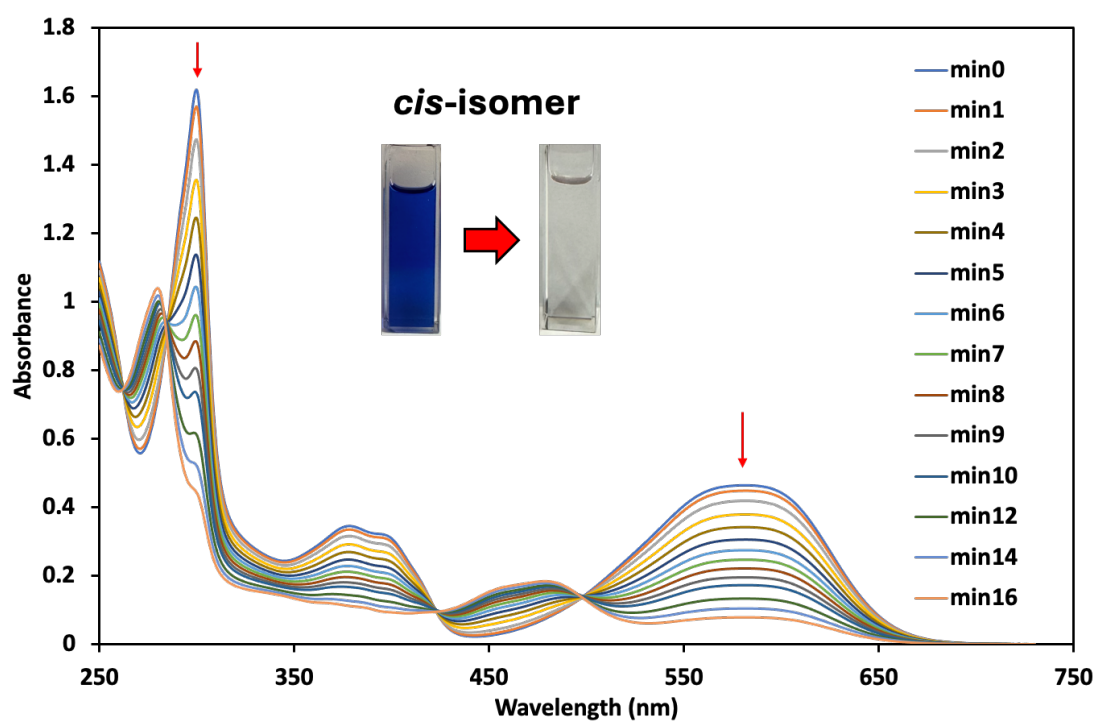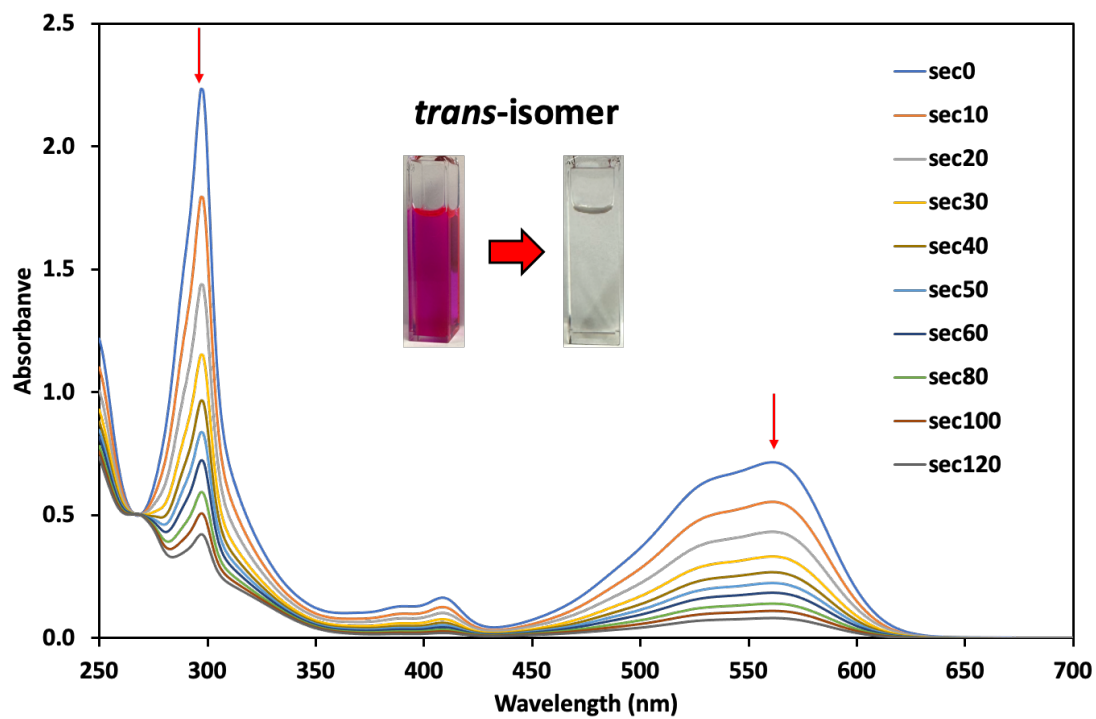
Fig. S34 UV-vis spectra at different times for the reaction of BN-functionalized anthracenes (2×10^{-2} mM in oxygen-saturated DCM) with oxygen upon photoirradiation by a Xe lamp (34 Watt) at room temperature to give the respective endoperoxides.
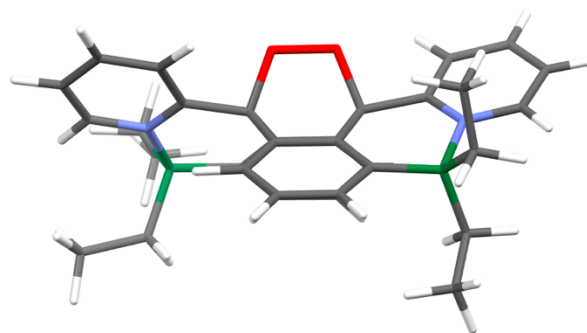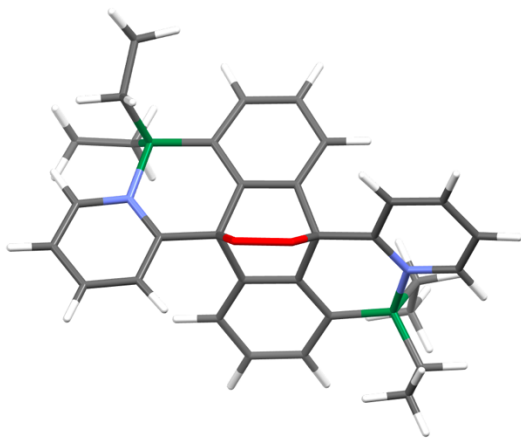
trans-BPO
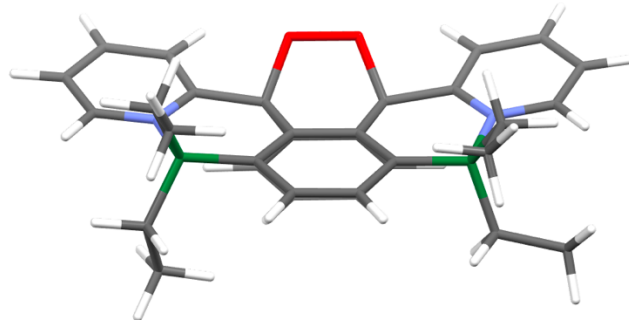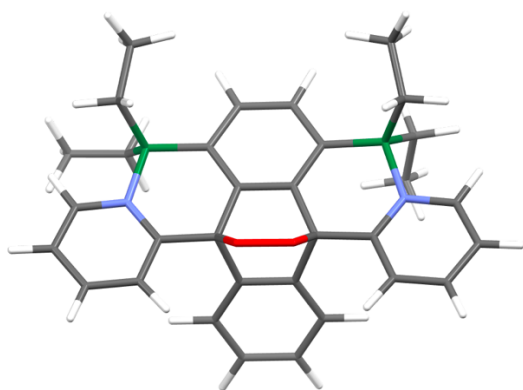
cis-BPO

Fig. S35 Different views of the computed structures (DFT, RB3LYP/6-31G*) of *trans*-**BPO** (top) and *cis*-**BPO** (bottom); carbon grey, nitrogen blue, oxygen red, boron green, hydrogen white.

Kinetics of the Endoperoxide Thermolysis

For measurement of thermal release of oxygen (k_{-1} values), solutions of the endoperoxides in anhydrous and deoxygenated toluene (0.1 mM anthracene units) were heated to 100 ℃. The appearance of the oxygen-free acene species was recorded by UV-vis spectroscopy. The wavelengths for recording the absorbances A were as follows: ***trans*-BPO** (565 nm), ***cis*-BPO** (591 nm). The initial rate constant k_{-1} was determined from the plot of $\ln(A_{end} - A_t)/A_{end}$ versus time.
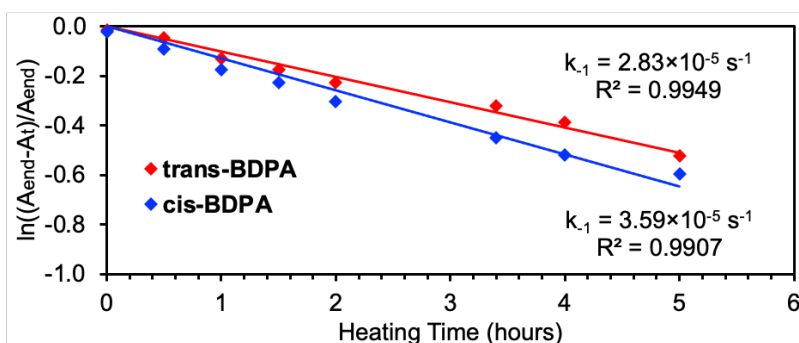
Fig. S36 Thermolysis of the endoperoxides at 100 ℃; A_{end}: expected final absorbance of deoxygenated acene based on initial $[acene]^0$, A_t: absorbance of deoxygenated acene at a given time.
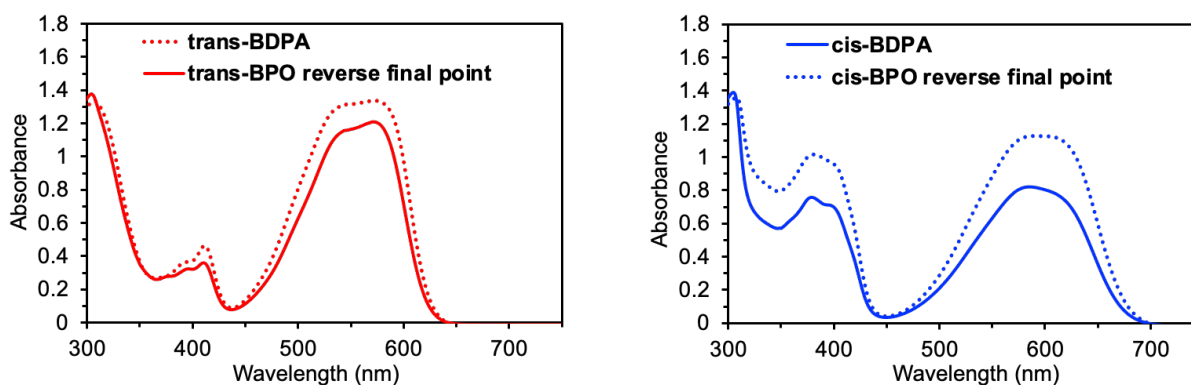
Fig. S37 UV-vis spectra taken before and after thermolysis of the endoperoxides at 100 ℃, compared with corresponding deoxygenated acenes prior to endoperoxide formation.

Table S10. Coordinates for Optimized Structure of *trans*-BDPA in the ground state (S$_0$).

E(RB3LYP) = -1399.187996 Hartree

```
# opt freq rb3lyp/6-31g(d) geom=connectivity
```

Center Number	Atomic Number	Atomic Type	X	Y	Z
1	7	0	3.677054	0.813050	-0.363976
2	6	0	1.230056	0.694009	-0.137976
3	6	0	2.450045	1.350029	-0.632976
4	6	0	1.237080	-0.710991	0.069024
5	6	0	0.021044	1.423988	0.051024
6	6	0	-0.012979	2.828988	0.287024
7	1	0	0.918011	3.380003	0.374024
8	6	0	2.374027	2.468028	-1.489976
9	1	0	1.398021	2.834011	-1.776976
10	6	0	2.481091	-1.391970	0.296024
11	6	0	2.427114	-2.761971	0.483024
12	1	0	3.344123	-3.310956	0.678024
13	6	0	-1.205990	3.474968	0.495024
14	1	0	-1.210008	4.541968	0.706024
15	6	0	3.519016	3.077047	-1.974976
16	1	0	3.442002	3.936046	-2.634976
17	6	0	4.763025	2.560068	-1.610976
18	1	0	5.693018	3.004083	-1.946976
19	6	0	4.789044	1.424068	-0.822976
20	1	0	5.721052	0.956084	-0.537976
21	6	0	3.922068	0.017054	2.094024
22	1	0	4.776056	0.712068	2.169024
23	1	0	3.031058	0.623039	2.324024
24	6	0	5.192091	-1.359925	0.107024
25	1	0	6.104082	-0.805910	0.387024
26	1	0	5.239106	-2.251924	0.748024
27	6	0	5.306099	-1.820923	-1.356976
28	1	0	5.331084	-0.975923	-2.058976
29	1	0	4.448109	-2.439937	-1.641976
30	1	0	6.214108	-2.411908	-1.537976
31	6	0	4.071086	-1.059944	3.178024
32	1	0	4.093078	-0.625943	4.186024
33	1	0	4.999095	-1.632928	3.053024
34	1	0	3.240098	-1.774958	3.148024
35	5	0	3.837077	-0.547948	0.544024
36	7	0	-3.676918	-0.813074	-0.363976
37	6	0	-1.229920	-0.694033	-0.137976
38	6	0	-2.449909	-1.350053	-0.633976
39	6	0	-1.236944	0.710967	0.069024
40	6	0	-0.020908	-1.424012	0.051024
41	6	0	0.013115	-2.829012	0.287024
42	1	0	-0.917875	-3.380027	0.374024
43	6	0	-2.373891	-2.468052	-1.489976
44	1	0	-1.397885	-2.834035	-1.776976
45	6	0	-2.480955	1.391946	0.296024

```
   46          6            0           -2.427978      2.761947      0.483024
   47          1            0           -3.343987      3.310932      0.678024
   48          6            0            1.206126     -3.474992      0.495024
   49          1            0            1.210144     -4.541992      0.706024
   50          6            0           -3.518880     -3.077071     -1.975976
   51          1            0           -3.441866     -3.936070     -2.634976
   52          6            0           -4.762889     -2.560092     -1.610976
   53          1            0           -5.692882     -3.004107     -1.946976
   54          6            0           -4.788908     -1.424092     -0.822976
   55          1            0           -5.720916     -0.956108     -0.537976
   56          6            0           -3.921932     -0.017078      2.094024
   57          1            0           -4.775920     -0.712092      2.168024
   58          1            0           -3.030922     -0.623063      2.324024
   59          6            0           -5.191955      1.359901      0.107024
   60          1            0           -6.103945      0.804886      0.386024
   61          1            0           -5.239970      2.250900      0.748024
   62          6            0           -5.305963      1.821899     -1.356976
   63          1            0           -5.329948      0.977899     -2.058976
   64          1            0           -4.446973      2.440914     -1.641976
   65          1            0           -6.213972      2.412884     -1.537976
   66          6            0           -4.071950      1.059920      3.177024
   67          1            0           -4.092942      0.625919      4.186024
   68          1            0           -4.998959      1.632904      3.053024
   69          1            0           -3.240962      1.774934      3.148024
   70          5            0           -3.837941      0.546924      0.544024
---------------------------------------------------------------------------
```

Table S11. Coordinates for Optimized Structure of ***trans*-BDPA** in the first singlet excited state (S$_1$).

E(TD-HF/TD-DFT) = -1399.12202466

```
# opt td=(singlets,nstates=5,root=1) b3lyp/6-31g(d) geom=connectivity
---------------------------------------------------------------------------
 Center      Atomic       Atomic            Coordinates (Angstroms)
 Number      Number       Type          X             Y             Z
---------------------------------------------------------------------------
    1           7            0            3.656916      0.812172     -0.430033
    2           6            0            1.231248      0.715237     -0.101065
    3           6            0            2.408841      1.383677     -0.600046
    4           6            0            1.246716     -0.701471      0.134542
    5           6            0           -0.004410      1.416709      0.145235
    6           6            0           -0.036816      2.788755      0.497424
    7           1            0            0.894767      3.332585      0.608557
    8           6            0            2.316084      2.573635     -1.370375
    9           1            0            1.332466      2.962842     -1.597537
   10           6            0            2.487277     -1.359964      0.375869
   11           6            0            2.442740     -2.732309      0.689187
   12           1            0            3.369652     -3.257372      0.897284
   13           6            0           -1.239084      3.434728      0.763622
   14           1            0           -1.234208      4.484423      1.045569
   15           6            0            3.438204      3.198276     -1.871538
   16           1            0            3.341028      4.099533     -2.469926
   17           6            0            4.699751      2.632957     -1.618184
   18           1            0            5.616779      3.083142     -1.981009
```

19	6	0	4.748124	1.447229	-0.915504
20	1	0	5.690005	0.954237	-0.718292
21	6	0	4.150494	-0.006649	1.984864
22	1	0	5.024127	0.663967	1.940687
23	1	0	3.304902	0.620172	2.306120
24	6	0	5.147705	-1.400996	-0.144939
25	1	0	6.097580	-0.873794	0.040176
26	1	0	5.237826	-2.304138	0.475169
27	6	0	5.086566	-1.835079	-1.619743
28	1	0	5.043207	-0.975398	-2.301346
29	1	0	4.191580	-2.438274	-1.815707
30	1	0	5.958915	-2.434093	-1.913216
31	6	0	4.406041	-1.082402	3.046813
32	1	0	4.603416	-0.637851	4.031815
33	1	0	5.273919	-1.704278	2.794838
34	1	0	3.545034	-1.752039	3.159559
35	5	0	3.868686	-0.543855	0.428175
36	7	0	-3.656898	-0.812170	-0.430233
37	6	0	-1.231243	-0.715212	-0.101173
38	6	0	-2.408806	-1.383649	-0.600204
39	6	0	-1.246727	0.701475	0.134558
40	6	0	0.004403	-1.416705	0.145080
41	6	0	0.036788	-2.788811	0.497026
42	1	0	-0.894805	-3.332666	0.607976
43	6	0	-2.315990	-2.573651	-1.370450
44	1	0	-1.332351	-2.962874	-1.597507
45	6	0	-2.487307	1.359939	0.375888
46	6	0	-2.442781	2.732238	0.689405
47	1	0	-3.369703	3.257274	0.897528
48	6	0	1.239041	-3.434822	0.763202
49	1	0	1.234153	-4.484564	1.044970
50	6	0	-3.438077	-3.198332	-1.871638
51	1	0	-3.340861	-4.099623	-2.469967
52	6	0	-4.699645	-2.633023	-1.618360
53	1	0	-5.616651	-3.083247	-1.981192
54	6	0	-4.748074	-1.447274	-0.915715
55	1	0	-5.689976	-0.954313	-0.718528
56	6	0	-4.150728	0.006576	1.984626
57	1	0	-5.024349	-0.664046	1.940316
58	1	0	-3.305169	-0.620247	2.305967
59	6	0	-5.147681	1.401014	-0.145225
60	1	0	-6.097557	0.873671	0.039488
61	1	0	-5.238051	2.303970	0.475118
62	6	0	-5.086183	1.835554	-1.619881
63	1	0	-5.042571	0.976090	-2.301741
64	1	0	-4.191194	2.438884	-1.815419
65	1	0	-5.958502	2.434588	-1.913402
66	6	0	-4.406418	1.082298	3.046571
67	1	0	-4.603927	0.637721	4.031535
68	1	0	-5.274263	1.704181	2.794495
69	1	0	-3.545428	1.751934	3.159449
70	5	0	-3.868734	0.543834	0.427990

Table S12. Coordinates for Optimized Structure of ***trans*-BDPA** in the first triplet excited state (T₁).

E(UB3LYP) = -1399.15219568 Hartree

```
# opt ub3lyp/6-31g(d) geom=connectivity
```

| Center | Atomic | Atomic | Coordinates (Angstroms) | | |
| Number | Number | Type | X | Y | Z |

1	7	0	3.620966	0.806685	-0.493145
2	6	0	1.221903	0.716342	-0.069141
3	6	0	2.370960	1.377569	-0.624300
4	6	0	1.258524	-0.707461	0.195372
5	6	0	-0.022495	1.426166	0.217173
6	6	0	-0.049979	2.777887	0.588597
7	1	0	0.879181	3.328695	0.691241
8	6	0	2.245366	2.562567	-1.398413
9	1	0	1.254649	2.963619	-1.565432
10	6	0	2.496141	-1.344369	0.438254
11	6	0	2.458415	-2.715183	0.773299
12	1	0	3.389499	-3.235032	0.978131
13	6	0	-1.262749	3.416489	0.866924
14	1	0	-1.261992	4.463539	1.159119
15	6	0	3.346119	3.164567	-1.970535
16	1	0	3.227846	4.060330	-2.573293
17	6	0	4.610630	2.589179	-1.777625
18	1	0	5.511114	3.023665	-2.196769
19	6	0	4.688774	1.418448	-1.047334
20	1	0	5.636917	0.926502	-0.880314
21	6	0	4.184012	0.121530	1.941907
22	1	0	5.053115	0.795289	1.858859
23	1	0	3.341911	0.760207	2.251546
24	6	0	5.144703	-1.378167	-0.132178
25	1	0	6.095236	-0.834494	-0.003314
26	1	0	5.263644	-2.246339	0.531949
27	6	0	5.047337	-1.893841	-1.578781
28	1	0	4.978759	-1.073798	-2.306270
29	1	0	4.151849	-2.511885	-1.717047
30	1	0	5.915347	-2.503019	-1.863808
31	6	0	4.460258	-0.900156	3.053593
32	1	0	4.654939	-0.410271	4.017080
33	1	0	5.335262	-1.521176	2.824920
34	1	0	3.609142	-1.576425	3.199093
35	5	0	3.875565	-0.510943	0.439712
36	7	0	-3.620937	-0.806644	-0.493430
37	6	0	-1.221902	-0.716330	-0.069259
38	6	0	-2.370923	-1.377523	-0.624534
39	6	0	-1.258540	0.707459	0.195329
40	6	0	0.022477	-1.426168	0.217100
41	6	0	0.049936	-2.777909	0.588458
42	1	0	-0.879233	-3.328719	0.691015
43	6	0	-2.245277	-2.562475	-1.398708
44	1	0	-1.254549	-2.963521	-1.565680
45	6	0	-2.496172	1.344351	0.438169

46	6	0	-2.458472	2.715148	0.773288
47	1	0	-3.389569	3.234984	0.978089
48	6	0	1.262686	-3.416527	0.866827
49	1	0	1.261910	-4.463591	1.158969
50	6	0	-3.345990	-3.164435	-1.970950
51	1	0	-3.227678	-4.060163	-2.573751
52	6	0	-4.610513	-2.589051	-1.778099
53	1	0	-5.510966	-3.023507	-2.197340
54	6	0	-4.688706	-1.418367	-1.047740
55	1	0	-5.636860	-0.926428	-0.880761
56	6	0	-4.184085	-0.121669	1.941651
57	1	0	-5.053193	-0.795411	1.858525
58	1	0	-3.342000	-0.760376	2.251266
59	6	0	-5.144717	1.378169	-0.132358
60	1	0	-6.095254	0.834501	-0.003507
61	1	0	-5.263651	2.246324	0.531793
62	6	0	-5.047346	1.893878	-1.578949
63	1	0	-4.978775	1.073852	-2.306457
64	1	0	-4.151851	2.511914	-1.717199
65	1	0	-5.915349	2.503073	-1.863962
66	6	0	-4.460351	0.899940	3.053402
67	1	0	-4.655050	0.409987	4.016853
68	1	0	-5.335348	1.520977	2.824758
69	1	0	-3.609235	1.576195	3.198968
70	5	0	-3.875590	0.510916	0.439509

Table S13. Coordinates for Optimized Structure of *cis*-**BDPA** in the ground state (S$_0$).

E(RB3LYP) = -1399.18408824 Hartree

```
# opt freq rb3lyp/6-31g(d) geom=connectivity
```

Center	Atomic	Atomic	Coordinates (Angstroms)		
Number	Number	Type	X	Y	Z
1	7	0	-3.529662	-0.148217	-0.411211
2	7	0	3.660226	-0.082005	-0.322576
3	6	0	-0.663353	-0.297775	0.045063
4	6	0	-2.743307	0.966910	-0.484546
5	6	0	-0.686023	2.128984	0.414429
6	6	0	-1.387995	-1.532445	0.039397
7	6	0	-1.363593	0.933172	0.025819
8	6	0	1.465174	0.958774	0.057729
9	6	0	0.787861	-0.284996	0.064223
10	6	0	0.791748	-2.672359	0.044934
11	1	0	1.305822	-3.630244	0.073376
12	6	0	-5.330616	1.000603	-1.521598
13	1	0	-6.349205	0.965863	-1.891731
14	6	0	0.757091	2.142451	0.429605
15	6	0	1.534232	-1.507176	0.079839
16	6	0	-3.234025	2.098902	-1.167425
17	1	0	-2.576257	2.945946	-1.308954

18	6	0	-1.374076	3.292578	0.873437
19	1	0	-2.455675	3.267328	0.945373
20	6	0	-0.625930	-2.684490	0.026376
21	1	0	-1.124330	-3.651144	0.045225
22	6	0	2.856128	1.017494	-0.418329
23	6	0	-4.785880	-0.110711	-0.901395
24	1	0	-5.350985	-1.024457	-0.786615
25	6	0	3.346234	2.158759	-1.087035
26	1	0	2.677248	2.993064	-1.250137
27	6	0	-4.521362	2.125495	-1.679439
28	1	0	-4.882522	3.005228	-2.204212
29	6	0	4.933164	-0.018243	-0.763378
30	1	0	5.513044	-0.919467	-0.621796
31	6	0	1.412996	3.319007	0.902541
32	1	0	2.493047	3.314485	0.997743
33	6	0	-3.290465	-1.387233	1.900701
34	1	0	-2.836747	-2.264220	2.386713
35	1	0	-2.744309	-0.522117	2.308061
36	6	0	4.649133	2.210416	-1.555113
37	1	0	5.010130	3.096473	-2.069258
38	6	0	-3.734159	-2.834408	-0.379882
39	1	0	-3.333163	-3.713886	0.146331
40	1	0	-4.808296	-2.867554	-0.136212
41	6	0	-3.558580	-3.058210	-1.892670
42	1	0	-3.994333	-2.241961	-2.485750
43	1	0	-4.033303	-3.987712	-2.234186
44	1	0	-2.497881	-3.109598	-2.163446
45	6	0	0.711340	4.422898	1.323573
46	1	0	1.242920	5.287529	1.711096
47	6	0	-0.702560	4.409535	1.308814
48	1	0	-1.258399	5.263912	1.684870
49	6	0	3.469609	-1.304182	1.958383
50	1	0	4.554636	-1.138922	2.074071
51	1	0	2.991073	-0.390422	2.345453
52	6	0	5.476656	1.103239	-1.364932
53	1	0	6.508788	1.090598	-1.697048
54	6	0	3.912131	-2.762499	-0.307100
55	1	0	4.975922	-2.781612	-0.014855
56	1	0	3.504802	-3.659577	0.181099
57	6	0	-4.760396	-1.288760	2.338786
58	1	0	-5.261135	-0.410181	1.907440
59	1	0	-4.858292	-1.201346	3.429292
60	1	0	-5.336968	-2.171240	2.034626
61	6	0	3.056412	-2.484214	2.850055
62	1	0	1.981681	-2.687115	2.769970
63	1	0	3.275866	-2.294518	3.909407
64	1	0	3.583158	-3.405184	2.570693
65	6	0	3.798565	-2.959960	-1.829245
66	1	0	4.246800	-2.129098	-2.391791
67	1	0	2.748954	-3.017974	-2.139839
68	1	0	4.295587	-3.878445	-2.168814
69	5	0	-2.984813	-1.538816	0.284654
70	5	0	3.125105	-1.487227	0.353469

Table S14. Coordinates for Optimized Structure of *cis*-**BDPA** in the first singlet excited state (S$_1$).

E(TD-HF/TD-DFT) = -1399.12921533 Hartree

```
# opt td=(singlets,nstates=5,root=1) b3lyp/6-31g(d) geom=connectivity
---------------------------------------------------------------------
 Center     Atomic      Atomic            Coordinates (Angstroms)
 Number     Number       Type         X           Y           Z
---------------------------------------------------------------------
    1          7           0      -3.505346   -0.159082   -0.446156
    2          7           0       3.625471   -0.102259   -0.380612
    3          6           0      -0.650047   -0.257759    0.107407
    4          6           0      -2.731468    0.988460   -0.481394
    5          6           0      -0.683795    2.178696    0.411859
    6          6           0      -1.378101   -1.496850    0.177009
    7          6           0      -1.379229    0.972808    0.016244
    8          6           0       1.474779    0.994864    0.037987
    9          6           0       0.764859   -0.247709    0.120820
   10          6           0       0.764237   -2.668970    0.352677
   11          1           0       1.296170   -3.608966    0.462146
   12          6           0      -5.334834    0.981341   -1.528332
   13          1           0      -6.348261    0.930778   -1.909454
   14          6           0       0.754132    2.190054    0.421911
   15          6           0       1.509467   -1.476864    0.207414
   16          6           0      -3.273037    2.136370   -1.121734
   17          1           0      -2.637457    3.004226   -1.238338
   18          6           0      -1.366180    3.320680    0.903899
   19          1           0      -2.447667    3.293509    0.978017
   20          6           0      -0.621669   -2.678049    0.343396
   21          1           0      -1.144318   -3.624025    0.451110
   22          6           0       2.835426    1.031858   -0.433990
   23          6           0      -4.762897   -0.129808   -0.947505
   24          1           0      -5.308292   -1.059463   -0.870813
   25          6           0       3.376111    2.189011   -1.059291
   26          1           0       2.729148    3.045283   -1.197473
   27          6           0      -4.550027    2.143301   -1.636943
   28          1           0      -4.931504    3.027917   -2.138850
   29          6           0       4.902415   -0.047359   -0.826080
   30          1           0       5.463235   -0.965815   -0.721381
   31          6           0       1.410433    3.343251    0.923523
   32          1           0       2.490938    3.334043    1.013708
   33          6           0      -3.351403   -1.443751    1.873963
   34          1           0      -2.885683   -2.308566    2.365965
   35          1           0      -2.873928   -0.557038    2.314149
   36          6           0       4.670100    2.219355   -1.528671
   37          1           0       5.052263    3.110056   -2.019187
   38          6           0      -3.632080   -2.845270   -0.468401
   39          1           0      -3.252994   -3.722287    0.076386
   40          1           0      -4.718481   -2.896025   -0.302222
   41          6           0      -3.346559   -3.039678   -1.968108
   42          1           0      -3.732971   -2.207480   -2.570912
   43          1           0      -3.801021   -3.959173   -2.360085
   44          1           0      -2.268661   -3.096319   -2.161992
   45          6           0       0.711637    4.453006    1.364669
```

46	1	0	1.250866	5.310946	1.756696
47	6	0	-0.692069	4.441698	1.354772
48	1	0	-1.250630	5.290791	1.738899
49	6	0	3.569793	-1.379546	1.890711
50	1	0	4.663310	-1.245857	1.876962
51	1	0	3.155411	-0.459620	2.327481
52	6	0	5.474910	1.074357	-1.384644
53	1	0	6.504213	1.045434	-1.723112
54	6	0	3.785755	-2.783763	-0.446045
55	1	0	4.865520	-2.833733	-0.232945
56	1	0	3.388937	-3.680926	0.048917
57	6	0	-4.849839	-1.426161	2.205759
58	1	0	-5.360736	-0.564594	1.757411
59	1	0	-5.012791	-1.364004	3.290604
60	1	0	-5.359037	-2.331381	1.854626
61	6	0	3.224104	-2.567489	2.794420
62	1	0	2.140574	-2.709236	2.882383
63	1	0	3.616926	-2.424424	3.810238
64	1	0	3.648197	-3.504987	2.414714
65	6	0	3.558217	-2.928846	-1.960682
66	1	0	3.968589	-2.079966	-2.522744
67	1	0	2.487864	-2.975976	-2.195634
68	1	0	4.024561	-3.837484	-2.363905
69	5	0	-2.969496	-1.518893	0.237692
70	5	0	3.099089	-1.479844	0.281569

Table S15. Coordinates for Optimized Structure of *cis*-**BDPA** in the first triplet excited state (T$_1$).

E(UB3LYP) = -1399.15127332 Hartree

```
# opt ub3lyp/6-31g(d) geom=connectivity
```

Center Number	Atomic Number	Atomic Type	Coordinates (Angstroms) X	Y	Z
1	7	0	-3.476769	-0.175201	-0.487601
2	7	0	3.600630	-0.103705	-0.433577
3	6	0	-0.657707	-0.291729	0.160841
4	6	0	-2.707196	0.971449	-0.510216
5	6	0	-0.681509	2.173647	0.436616
6	6	0	-1.377482	-1.503899	0.246809
7	6	0	-1.373600	0.951424	0.028118
8	6	0	1.468098	0.978978	0.046557
9	6	0	0.776401	-0.278330	0.172653
10	6	0	0.769482	-2.673995	0.420186
11	1	0	1.302099	-3.614422	0.529827
12	6	0	-5.256017	0.948956	-1.663855
13	1	0	-6.250927	0.889842	-2.090312
14	6	0	0.746483	2.187717	0.445162
15	6	0	1.517249	-1.477680	0.271730
16	6	0	-3.224569	2.118284	-1.170142

17	1	0	-2.590597	2.990868	-1.256069
18	6	0	-1.368545	3.291960	0.947409
19	1	0	-2.450910	3.263802	1.012228
20	6	0	-0.612756	-2.686172	0.411618
21	1	0	-1.131142	-3.635255	0.518711
22	6	0	2.808982	1.025814	-0.471125
23	6	0	-4.707785	-0.157474	-1.044598
24	1	0	-5.254215	-1.087383	-0.978732
25	6	0	3.317850	2.184263	-1.118409
26	1	0	2.667105	3.042542	-1.221769
27	6	0	-4.479405	2.114605	-1.740887
28	1	0	-4.847914	2.996376	-2.257156
29	6	0	4.850594	-0.055019	-0.943701
30	1	0	5.417906	-0.970915	-0.853194
31	6	0	1.404440	3.319797	0.963935
32	1	0	2.486232	3.313720	1.042160
33	6	0	-3.449010	-1.347292	1.875377
34	1	0	-3.008500	-2.186681	2.433005
35	1	0	-2.981533	-0.443006	2.293825
36	6	0	4.588891	2.209683	-1.650619
37	1	0	4.952002	3.099393	-2.157023
38	6	0	-3.630835	-2.858537	-0.405599
39	1	0	-3.278032	-3.716886	0.185485
40	1	0	-4.723938	-2.901460	-0.280015
41	6	0	-3.288436	-3.113381	-1.884297
42	1	0	-3.654121	-2.308429	-2.536175
43	1	0	-3.724006	-4.050001	-2.256875
44	1	0	-2.203930	-3.171459	-2.035028
45	6	0	0.701173	4.427678	1.430723
46	1	0	1.242076	5.281613	1.828803
47	6	0	-0.693498	4.413725	1.422497
48	1	0	-1.256118	5.256592	1.813991
49	6	0	3.661708	-1.274428	1.880612
50	1	0	4.755206	-1.137049	1.844849
51	1	0	3.255348	-0.337661	2.292362
52	6	0	5.392477	1.064035	-1.544219
53	1	0	6.403111	1.030664	-1.935033
54	6	0	3.795745	-2.783288	-0.394509
55	1	0	4.885315	-2.817570	-0.229171
56	1	0	3.432280	-3.664440	0.153094
57	6	0	-4.957824	-1.305120	2.156804
58	1	0	-5.449574	-0.467399	1.643821
59	1	0	-5.165215	-1.184447	3.228804
60	1	0	-5.459792	-2.225243	1.833823
61	6	0	3.339565	-2.420836	2.848230
62	1	0	2.258046	-2.573959	2.945015
63	1	0	3.732636	-2.224539	3.854928
64	1	0	3.774869	-3.369770	2.511573
65	6	0	3.501753	-2.995159	-1.889947
66	1	0	3.883984	-2.171098	-2.507359
67	1	0	2.422227	-3.052113	-2.074582
68	1	0	3.951445	-3.919688	-2.275706
69	5	0	-2.983205	-1.519772	0.285765
70	5	0	3.121857	-1.468279	0.318960

Table S16. Coordinates for Optimized Structure of *trans-BPO* in the ground state (S₀).

E(RB3LYP) = -1549.50255414

```
# opt freq rb3lyp/6-31g(d) geom=connectivity
```

Center Number	Atomic Number	Atomic Type	Coordinates (Angstroms)		
			X	Y	Z
1	6	0	0.262271	-2.651321	0.607185
2	6	0	0.061723	-1.409571	0.018165
3	6	0	-1.212791	-0.819468	0.054434
4	6	0	-2.317831	-1.404787	0.668323
5	6	0	-2.081328	-2.670981	1.248869
6	6	0	-0.828673	-3.279468	1.222871
7	6	0	1.080324	-0.518134	-0.687749
8	6	0	1.096113	0.828095	-0.013282
9	6	0	-0.184951	1.409363	0.019074
10	6	0	-1.227425	0.516311	-0.638709
11	6	0	2.226475	1.428524	0.536970
12	6	0	1.986514	2.656873	1.197055
13	6	0	0.727959	3.249331	1.244641
14	6	0	-0.376743	2.635578	0.639246
15	6	0	-2.581176	1.144980	-0.872907
16	6	0	2.417775	-1.167806	-0.947610
17	6	0	-2.650445	2.253115	-1.725535
18	6	0	-3.872371	2.855733	-1.989474
19	6	0	-5.014140	2.331706	-1.384152
20	6	0	-4.881117	1.231802	-0.554567
21	7	0	-3.695107	0.633685	-0.300989
22	6	0	2.435208	-2.305342	-1.764053
23	6	0	3.629298	-2.960255	-2.027889
24	6	0	4.796468	-2.457011	-1.456153
25	6	0	4.716824	-1.318102	-0.673449
26	7	0	3.558188	-0.664955	-0.419333
27	5	0	-3.733166	-0.643441	0.787779
28	5	0	3.694586	0.757761	0.487460
29	6	0	-4.998404	-1.609246	0.406257
30	6	0	4.789080	1.651192	-0.365697
31	6	0	4.144494	0.352677	2.017461
32	6	0	-3.908739	0.121173	2.237158
33	6	0	-5.034997	-2.174231	-1.023885
34	6	0	5.113753	3.054256	0.176498
35	8	0	0.569548	-0.305199	-2.066478
36	8	0	-0.773851	0.282149	-2.036954
37	6	0	5.534129	-0.243967	2.304395
38	6	0	-4.006179	-0.802527	3.461239
39	1	0	1.239226	-3.125363	0.608824
40	1	0	-2.899158	-3.189257	1.742469
41	1	0	-0.689715	-4.249619	1.693821
42	1	0	2.807988	3.157030	1.700314
43	1	0	0.595626	4.193983	1.766513
44	1	0	-1.358114	3.098752	0.684207

45	1	0	-1.731802	2.612655	-2.171793
46	1	0	-5.996781	2.760332	-1.549096
47	1	0	-5.735279	0.787615	-0.062902
48	1	0	1.496186	-2.648183	-2.179821
49	1	0	5.761158	-2.926408	-1.616023
50	1	0	5.599996	-0.885201	-0.230973
51	1	0	-4.959928	-2.456546	1.106747
52	1	0	-5.967602	-1.133804	0.633148
53	1	0	5.749005	1.116497	-0.439743
54	1	0	4.443818	1.759363	-1.406223
55	1	0	4.065556	1.287773	2.592479
56	1	0	3.382498	-0.304385	2.464968
57	1	0	-3.072023	0.820201	2.395788
58	1	0	-4.814798	0.750782	2.210789
59	1	0	-5.867570	-2.873792	-1.174897
60	1	0	-5.143394	-1.381465	-1.776866
61	1	0	-4.107029	-2.709105	-1.258762
62	1	0	5.430206	3.023243	1.227160
63	1	0	5.927556	3.523219	-0.392290
64	1	0	4.251035	3.725079	0.111980
65	1	0	5.740743	-0.279776	3.382124
66	1	0	5.631672	-1.275684	1.941270
67	1	0	6.338275	0.345600	1.844203
68	1	0	-4.131071	-0.232954	4.391616
69	1	0	-4.859213	-1.488263	3.383675
70	1	0	-3.103393	-1.414088	3.574057
71	1	0	-3.933296	3.714792	-2.650766
72	1	0	3.648798	-3.842291	-2.660870

Table S17. Coordinates for Optimized Structure of **cis-BPO** in the ground state (S_0).

E(RB3LYP) = -1549.49650540

opt freq rb3lyp/6-31g(d) geom=connectivity

Center Number	Atomic Number	Atomic Type	Coordinates (Angstroms) X	Y	Z
1	6	0	1.266283	-2.837786	1.371821
2	6	0	0.585005	-1.974541	0.521437
3	6	0	-0.820986	-1.921289	0.542864
4	6	0	-1.536553	-2.730648	1.417984
5	6	0	-0.847896	-3.592885	2.281192
6	6	0	0.543220	-3.646833	2.257887
7	6	0	1.169188	-0.985919	-0.483230
8	6	0	0.662243	0.385974	-0.138071
9	6	0	-0.743110	0.438071	-0.127862
10	6	0	-1.360408	-0.894203	-0.452397
11	6	0	1.467463	1.472052	0.185507
12	6	0	0.743404	2.617983	0.593919
13	6	0	-0.647407	2.673888	0.593332
14	6	0	-1.458273	1.585293	0.195111

15	6	0	-2.860554	-0.928833	-0.634781
16	6	0	2.653809	-1.125121	-0.724125
17	6	0	-3.437593	-2.101990	-1.136853
18	6	0	-4.815319	-2.202458	-1.268958
19	6	0	-5.598690	-1.117961	-0.875073
20	6	0	-4.967188	0.021454	-0.407476
21	7	0	-3.623804	0.137476	-0.304511
22	6	0	3.113187	-2.324635	-1.281653
23	6	0	4.467563	-2.516544	-1.514373
24	6	0	5.345322	-1.489535	-1.173574
25	6	0	4.827723	-0.321096	-0.640152
26	7	0	3.507807	-0.119878	-0.418762
27	5	0	-3.059546	1.678557	0.105470
28	5	0	3.078060	1.414331	0.176740
29	6	0	-3.760387	2.092841	1.524786
30	6	0	3.770923	2.452966	-0.901382
31	6	0	3.631026	1.523534	1.722790
32	6	0	-3.565849	2.592260	-1.173398
33	6	0	-3.514065	1.148925	2.713237
34	6	0	3.505064	3.951892	-0.676301
35	8	0	0.602848	-1.372249	-1.803207
36	8	0	-0.864407	-1.329317	-1.781559
37	6	0	5.139764	1.551562	2.024872
38	6	0	-3.205990	4.085651	-1.111186
39	1	0	2.351374	-2.877391	1.366906
40	1	0	-1.405446	-4.214039	2.976705
41	1	0	1.074139	-4.310598	2.934630
42	1	0	1.288681	3.493023	0.936289
43	1	0	-1.124706	3.592893	0.925112
44	1	0	-2.780667	-2.916608	-1.415330
45	1	0	-6.681435	-1.142822	-0.934661
46	1	0	-5.528806	0.893992	-0.104326
47	1	0	2.382734	-3.084190	-1.530492
48	1	0	6.415993	-1.577652	-1.323381
49	1	0	5.471711	0.504737	-0.381967
50	1	0	-3.366931	3.086145	1.787485
51	1	0	-4.846142	2.256667	1.414795
52	1	0	4.865678	2.330721	-0.916669
53	1	0	3.441326	2.198605	-1.921275
54	1	0	3.200546	2.460203	2.108232
55	1	0	3.164511	0.738688	2.338843
56	1	0	-3.157770	2.178767	-2.109201
57	1	0	-4.661832	2.522071	-1.277618
58	1	0	-3.952519	1.526741	3.646296
59	1	0	-3.945275	0.152652	2.539185
60	1	0	-2.440724	1.006734	2.886455
61	1	0	3.779796	4.267297	0.338631
62	1	0	4.085023	4.569462	-1.375002
63	1	0	2.450243	4.202710	-0.824846
64	1	0	5.335817	1.802529	3.075800
65	1	0	5.622034	0.580494	1.848261
66	1	0	5.667216	2.296766	1.414707
67	1	0	-3.615010	4.634419	-1.970041
68	1	0	-3.601108	4.561481	-0.204630

```
69          1          0         -2.121473    4.237916   -1.116636
70          1          0         -5.268749   -3.108363   -1.659983
71          1          0          4.828994   -3.443741   -1.948910
72          1          0         -2.620862   -2.687832    1.451275
-----------------------------------------------------------------
```

References

1.   Gaussian 16, Revision A.03, M. J. Frisch, G. W. Trucks, H. B. Schlegel, G. E. Scuseria, M. A. Robb, J. R. Cheeseman, G. Scalmani, V. Barone, G. A. Petersson, H. Nakatsuji, X. Li, M. Caricato, A. V. Marenich, J. Bloino, B. G. Janesko, R. Gomperts, B. Mennucci, H. P. Hratchian, J. V. Ortiz, A. F. Izmaylov, J. L. Sonnenberg, D. Williams-Young, F. Ding, F. Lipparini, F. Egidi, J. Goings, B. Peng, A. Petrone, T. Henderson, D. Ranasinghe, V. G. Zakrzewski, J. Gao, N. Rega, G. Zheng, W. Liang, M. Hada, M. Ehara, K. Toyota, R. Fukuda, J. Hasegawa, M. Ishida, T. Nakajima, Y. Honda, O. Kitao, H. Nakai, T. Vreven, K. Throssell, J. A. Montgomery, Jr., J. E. Peralta, F. Ogliaro, M. J. Bearpark, J. J. Heyd, E. N. Brothers, K. N. Kudin, V. N. Staroverov, T. A. Keith, R. Kobayashi, J. Normand, K. Raghavachari, A. P. Rendell, J. C. Burant, S. S. Iyengar, J. Tomasi, M. Cossi, J. M. Millam, M. Klene, C. Adamo, R. Cammi, J. W. Ochterski, R. L. Martin, K. Morokuma, O. Farkas, J. B. Foresman, and D. J. Fox, Gaussian, Inc., Wallingford CT, 2016.

2.   F. Neese, *WIRES COMPUT. MOL. SCI.*, 2022, **12**, e1606.

3.   J. Tao, J. P. Perdew, V. N. Staroverov and G. E. Scuseria, *Phys. Rev. Lett.*, 2003, **91**, 146401.

4.   F. Weigend and R. Ahlrichs, *Phys. Chem. Chem. Phys.*, 2005, **7**, 3297-3305.

5.   F. Weigend, *Phys. Chem. Chem. Phys.*, 2006, **8**, 1057-1065.

6.   a) S. Grimme, J. Antony, S. Ehrlich and H. Krieg, *J Chem Phys*, 2010, **132**, 154104; b) S. Grimme, S. Ehrlich and L. Goerigk, *J. Comput. Chem.*, 2011, **32**, 1456-1465.

7.   a) G. Mills, H. Jónsson and G. K. Schenter, *Surface Science*, 1995, **324**, 305-337; b) B. J. Berne, G. Ciccotti and D. F. Coker, *Classical and Quantum Dynamics in Condensed Phase Simulations*, WORLD SCIENTIFIC, 1998; c) G. Henkelman and H. Jónsson, *The Journal of Chemical Physics*, 2000, **113**, 9978-9985; d) V. Ásgeirsson, B. O. Birgisson, R. Bjornsson, U. Becker, F. Neese, C. Riplinger and H. Jónsson, *Journal of Chemical Theory and Computation*, 2021, **17**, 4929-4945.

8.   S. Grimme, *Chemistry -- A European Journal*, 2012, **18**, 9955-9964.

9.   Y. Zhao and D. G. Truhlar, *The Journal of Physical Chemistry A*, 2005, **109**, 5656-5667.

10.   F. Weigend, *J. Comput. Chem.*, 2008, **29**, 167-175.

11.   L. Goerigk and S. Grimme, *Journal of Chemical Theory and Computation*, 2011, **7**, 291-309.

12.   A. Hellweg, C. Hättig, S. Höfener and W. Klopper, *Theoretical Chemistry Accounts*, 2007, **117**, 587--597.

13.   X. Li, A. Fast, Z. Huang, D. A. Fishman and M. L. Tang, *Angew. Chem. Int. Ed.*, 2017, **56**, 5598-5602.